

AD-A088 904

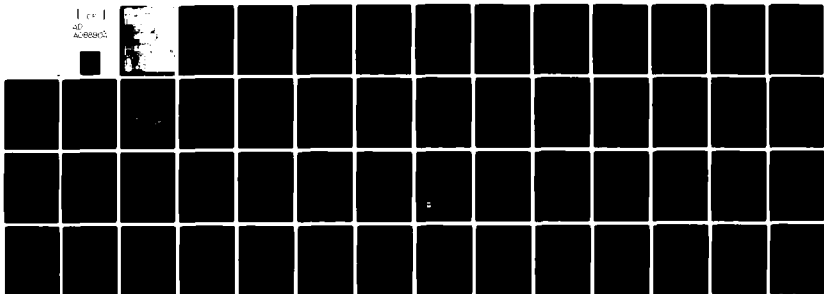
NAVAL RESEARCH LAB WASHINGTON DC  
APPLICATION OF PICOSECOND AND LIGHT SCATTERING SPECTROSCOPIES T--ETC(U)  
SEP 80 J N SCHNUR  
NRL-MR-4323

F/8 20/5

UNCLASSIFIED

NL

1 of 1  
of  
Accession



END  
DATE  
FILMED  
10-80  
DTIC

AD A088904



CONTENTS

Introduction..... 1

I. High-Power Picosecond Photolysis of Simple Organic Molecular Gases  
 B. B. Craig, W. L. Faust, L. S. Goldberg, J. M. Schnur,  
 P. E. Schoen and R. G. Weiss..... 5

II. Brillouin Scattering of Solithane 113 at High Pressure  
 M. Abebe and P. E. Schoen..... 19

III. Application of Advanced Optical Spectroscopic Methods to  
 Energetic Materials  
 L. S. Goldberg, J. M. Schnur, P. E. Schoen, W. L. Faust,  
 T. R. Royt, S. Wunder and M. Abebe..... 31

IV. Application of Advanced Light Scattering Techniques to the Study  
 of Polymer Properties  
 J. M. Schnur, P. Schoen and S. L. Wunder..... 40

Author	
Title	
Institution	
Availability Codes	
Unavail and/or Special	
	

# APPLICATION OF PICOSECOND AND LIGHT SCATTERING SPECTROSCOPIES TO THE STUDY OF ENERGETIC MATERIALS

## Summary Report

### INTRODUCTION

This report describes recent progress in NRL's research involving the application of advanced spectroscopies to the study of energetic materials. This program is currently jointly funded by the Office of Naval Research (project #RR0240202) DARPA (project #3702) as well as by NRL's in house core basic research program.

The goal of this research is to identify advanced optical procedures appropriate for the study of energetic materials and their reactions, develop these techniques as required, assess their utility to the energetic material community, and then aid in the transfer of the appropriate technology to the appropriate user groups.

Previous reports have detailed the development of light scattering techniques to study material properties at high pressures. The successful application of this method to the study of complex material problems has recently led to the initiation of two distinct research programs.

These are (A) the application of high pressure Raman, FTIR, and Brillouin techniques to study the role of supra molecular structure in determining material strength in polyethelene (now supported by NAVAIR) and (B) the application of high pressure Raman and FTIR in determining the possible effect of pressure in catalyzing decomposition in NOS-365 and other monopropellents. (Now supported by NAVSEA).

Concurrent with ONR supported light scattering program, NRL has been developing the technology of ultrafast, ultrahigh power lasers. During the past year ONR and DARPA have supported (along with NRL) a program to determine the utility of applying these ultrafast techniques to the study of energetic materials and their reactions.

Manuscript submitted June 30, 1980

As a result of developments in picosecond sources and detection systems, NRL's energetic materials program now incorporates both picosecond spectroscopy and light scattering techniques in its studies of energetic materials.

The research in both these problem areas has been quite productive since the last report. Recent results are summarized below and the resulting manuscripts and publications follow this introduction.

A. High-power picosecond pulse lasers are being developed and utilized to initiate the primary events of ultrafast reactions in energetic materials. These sources are being applied (under ONR and DARPA support) to characterize both condensed phase and gaseous photo-induced reactions. By application of state-of-the-art, ultrafast spectroscopic techniques it is now possible to observe the earliest species produced in ultrafast reactions, i.e. products formed within ca. 10 picoseconds after laser initiation. It is anticipated that such information will provide a better understanding of deflagration-to-detonation transitions. Also under experimental study is an assessment of the feasibility of modifying energetic reactions by perturbation of the initial reaction pathways.

These experiments at NRL are in collaboration with photochemists from Georgetown University. In this past year, we have carried out a series of new experiments to study the photodissociation of simple hydrocarbons and nitro bearing molecules under conditions of intense picosecond UV irradiation and high gaseous pressures. Our interest is in the decomposition of simple compounds which afford generic models for processes important in explosives, fuels, and other energetic materials.

The time definition inherent in picosecond pulse excitation enables the near-instantaneous deposition of energy into the molecular system, before secondary reactions or collisions can ensue. We are employing an excitation mechanism that is nonspecific in the molecule it addresses, thereby facilitating the decomposition of a wide variety of materials. The mechanism involves multiphoton absorption and laser-induced dielectric breakdown processes that are attendant at the high laser flux density ( $>10^{11}$  W/cm<sup>2</sup>) and pressures (10-500 torr) of our experiments.

We have irradiated gaseous samples of ketene, methane, protonated and deuterated nitromethane, and carbon monoxide and have observed visible emission originating from electronically-excited fragment products. High-resolution spectral and temporal studies of the dominant emitting fragments, C<sub>2</sub>, CH, CN and H, show emission characteristics that depend strongly upon the parent molecule under irradiation. For example, C<sub>2</sub> emission derived from ketene and methane bears a high degree of rotational excitation and exhibits a risetime that currently is detection-limited at below a nanosecond; when derived from carbon monoxide, however, the C<sub>2</sub> emitting population is rotationally cooler

and develops and decays collisionally over a period of microseconds. The mechanism by which  $C_2$  is formed from methane must of necessity be a (rapid) collisional process, though clearly different in nature to that for carbon monoxide, whereas ketene ( $CH_2CO$ ) could support a unimolecular dissociative formation of  $C_2$  through elimination of H and O atoms. Improved time-dependent emission data from our ongoing measurements should yield a clearer understanding of the possible reaction pathways involved in these dissociative processes. The further application of these techniques to nitro bearing alkanes and other related compounds may provide important information on reactions through which these molecules communicate in the early phases of rapid decomposition.

We will also be extending our probe measurements to study the composition and dynamics of the nonemissive, ground-state fragment population. This will utilize our already established capability to obtain picosecond transient absorption spectra and will introduce a new picosecond probe technique of laser induced fluorescence. The latter method, which is based on time-synchronized excitation of ground-state products by a synchronously-modelocked tunable dye laser, should enable probing for reactive intermediates such as the methylene radical,  $CH_2$ . We are also exploring coherent Raman vibrational probing as a means of opening a far greater class of molecular fragment species to investigation.

These initial experiments have resulted in the characterization of excitation of nitromethane and ketene and the subsequent identification of some of their resulting primary products. The ability to identify the important primary products in fast energetic reactions is critical to the understanding of complete reaction mechanisms. Future investigations will include more complex energetic materials such as HMX and RDX. As these experiments proceed, and the primary kinetic events are elucidated, attempts to modify the kinetics will be made.

B. Brillouin spectroscopy is being applied to the characterization of cross-linked polymeric materials as part of an ONR program to determine the relationship of molecular structure to macroscopic properties. NRL's contribution to the ONR program is the measurement of the high-frequency viscoelastic moduli as a function of temperature and pressure. This is accomplished by utilizing NRL's recently developed high-pressure light scattering spectroscopic techniques.

This program of collaborative research has been established so that a single model polymer binder, Solithane 113, can be characterized in detail by the various techniques of the cooperating groups. In this way a complete picture can be constructed of the response of a specific binder to a range of stresses.

As part of this effort NRL has performed Brillouin scattering measurements of the viscoelastic moduli of Solithane at a frequency of ~10 GHz. This frequency range is orders of magnitude higher than pre-

viously utilized with binders. Recent theoretical work has indicated that the very high frequency response of these materials bears significantly upon their ability to resist fracture. Another consideration is the Williams-Landel-Ferry principle i.e. that for polymers there is an equivalence between the variables time, pressure and temperature: that the response of a polymer to mechanical stress at lower temperatures is related to its response at higher pressures, which is also related to its shorter time (higher frequency) behavior. The question we are addressing is over what range of times, temperatures and pressures these equivalences hold.

During the past year we have successfully determined the longitudinal elastic moduli of Solithane in the gigahertz frequency range. The moduli (or compressive stiffnesses) were obtained as functions of frequency and pressure and were compared with lower frequency ultrasonic (1Mhz) data. The primary conclusions to be drawn from this work are that 1) such measurements are indeed feasible, and 2) the moduli of the model compound become much stiffer (i.e., more brittle or glassy) at high frequencies and high pressures. This is a fact which must be taken into consideration when more realistic binder polymers are chosen to serve as the shock absorbing matrix holding energetic material.

We are now undertaking to examine in more depth the interrelationships between the variables pressure, temperature, and frequency and the conditions under which they are equivalent. We shall examine further the pressure and temperature behavior of Solithane in the gigahertz regime and investigate the effect of systematic variations in polymer composition and plasticization.

## HIGH-POWER PICOSECOND PHOTOLYSIS OF SIMPLE ORGANIC MOLECULAR GASES<sup>†</sup>

B.B. Craig\*, W.L. Faust, L.S. Goldberg, J.M. Schnur,  
P.E. Schoen and R.G. Weiss\*

Naval Research Laboratory, Washington, D.C. 20375, U.S.A.

\*Department of Chemistry, Georgetown University,  
Washington, D.C. 20057, U.S.A.

### ABSTRACT

High-power picosecond UV pulses from a Nd:YAG modelocked laser were used to induce a visible emission from a variety of gaseous organic molecules. We report the observation of electronically excited  $C_2$ , CH, CN and H fragments. The spectral characteristics and time development of the emitting species are highly dependent upon the structure of the parent molecules.

### INTRODUCTION

Laser photolysis of simple molecules has contributed to a deeper understanding of dynamical processes in photodissociation. Our concern in the present work is with the decomposition of simple compounds which afford generic models of processes important in explosives, fuels and other energetic materials. Multiphoton IR and UV laser dissociation (1-4) has previously been applied to study the primary decomposition processes of gas-phase hydrocarbons and subsequent reaction of fragments having significance in the kinetics of combustion. These experiments have been performed in the nanosecond time domain and at millitorr gas pressures in order to maintain a collision-free time regime during the duration of the excitation pulse. In our experiments the time resolution afforded by picosecond pulse excitation enables such photolysis even at atmospheric pressures, yielding high fragment concentrations. For the pressures and high flux densities employed in this work, multiphoton absorption processes can be accompanied by dielectric breakdown (5). Indeed, since laser-induced breakdown is a non-resonant process, this very non-specificity facilitates the decomposition of a wide variety of materials.

Here, we demonstrate the utility of the technique in generating fragments whose emission spectra reflect their precursors. We have carried out the photolysis of ketene, methane, carbon monoxide and nitromethane at pressures in the range of 10-500 torr, and studied the luminescence from  $C_2$ , CH, CN and H fragments.

## EXPERIMENTAL

Figure 1 shows a schematic of the Nd:YAG laser system. The flashlamp-pumped oscillator, operating at a 1 Hz repetition rate, employed a hybrid modelocking approach to provide more reproducible pulse-train generation. It utilized an active acousto-optic loss modulator (Quantronix) and a passive saturable absorbing dye (Eastman A9740) in a flow cell. The single 1064 nm pulse, switched from near the peak of the train, had ca. 0.4 mJ energy and typically 30 ps duration. Two stages of amplification, apodization and spatial filtering of the beam provided a high-spatial-quality IR pulse of 30-40 mJ energy. Efficient frequency doubling and redoubling in KD\*P crystals generated a 4th harmonic (266 nm) photolyzing pulse of up to 10 mJ energy. The laser beam was focused to a 0.15 mm spot diameter in a static gas cell (ca. 100 cm<sup>3</sup>) through a LiF window. The emitted light generated from individual laser shots was collected at right angles and focused into a grating monochromator coupled to a Nuclear Data ND100 intensified vidicon multi-channel recording system (spectral sensitivity 380-800 nm). Improved signal-to-noise was achieved where necessary by accumulating data from typically 30 laser shots. High-resolution spectra were obtained with a Spex 0.8 m monochromator (0.1 nm system resolution). For time-resolved studies, a Varian VPM-154M cross-field photomultiplier was coupled to the exit slit of the monochromator. The transient signal was displayed on a Tektronix 7104 oscilloscope, giving a detection risetime of 400 ps. Observations were also made with an Electrophotonics streak camera (S-20 photocathode) having time resolution of 10 ps.

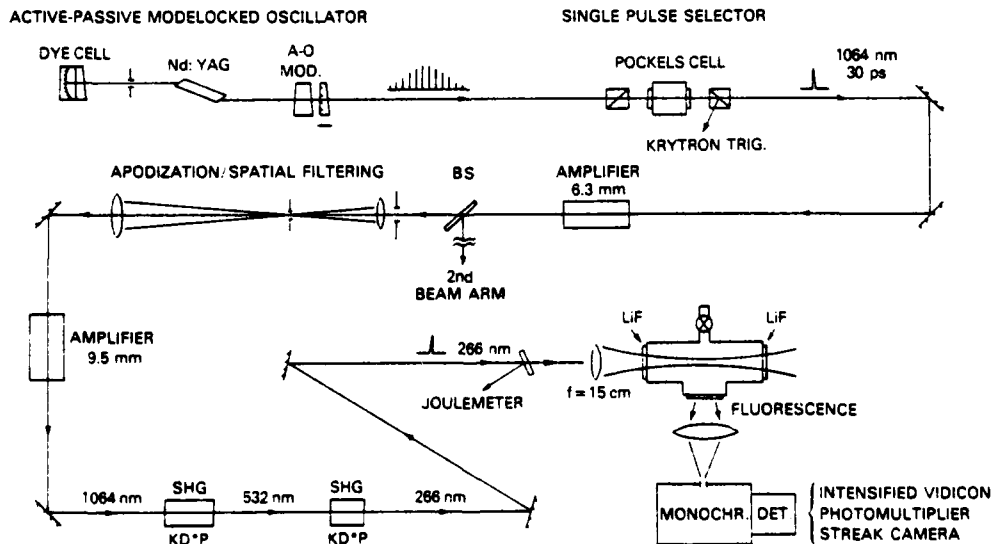


Fig. 1. Schematic of the laser system.

Methane was research grade purity supplied by Matheson Gas Products and was used without further purification. Carbon monoxide was ultra-high purity grade (Matheson) and was freed of any metal carbonyl contaminants by passing through a heated tube (200°C, atmospheric pressure) packed with glass wool (6). Nitromethane was Baker reagent grade and was distilled under nitrogen, collecting the middle fraction, b.p. 101-102°C. Ketene, CH<sub>2</sub>CO, was prepared by a standard procedure (7) involving dehydration of acetic anhydride at 500-550°C and was purified by trap-to-trap distillation. It was stored in the dark under vacuum in a liquid nitrogen bath. A salt-ice bath placed between the reservoir and sample cell was used to condense traces of acetic acid and other high-boiling impurities.

## RESULTS AND DISCUSSION

High-power, 30 ps pulses at 266 nm focused into the vapors under study (10-500 torr) generated a visible streak near the focal region. Low- and high-resolution spectra of the luminescence exhibited no differences in intensity or spectral distribution during a typical experiment involving several hundred laser shots. This indicates that stable photolytic products do not significantly affect the primary decomposition processes. The result is not surprising since the photolysed region is at least 10<sup>9</sup> smaller than the total sample volume. It should be emphasized that our analytical techniques give evidence only of luminescent species; other intermediates are undoubtedly produced.

Figure 2 depicts the similarity of the low-resolution emission spectra from ketene and carbon monoxide, each at 100 torr. High-resolution spectra indicate that the <sub>3</sub>predominant emission belongs to the C<sub>2</sub> diradical in its triplet d<sup>3</sup>Π → a<sup>3</sup>Π Swan transition (8). Figures 3 and 4 show the Δv = 0 and Δv = -1 transitions for C<sub>2</sub> from carbon monoxide, methane and ketene. The emission spectra from methane and ketene exhibit a strong attendant rotational structure. In addition, a weak, underlying continuum emission, associated with a plasma formation, extended throughout the visible region. The intensity of this background varied for each gas studied but was most prominent for methane.

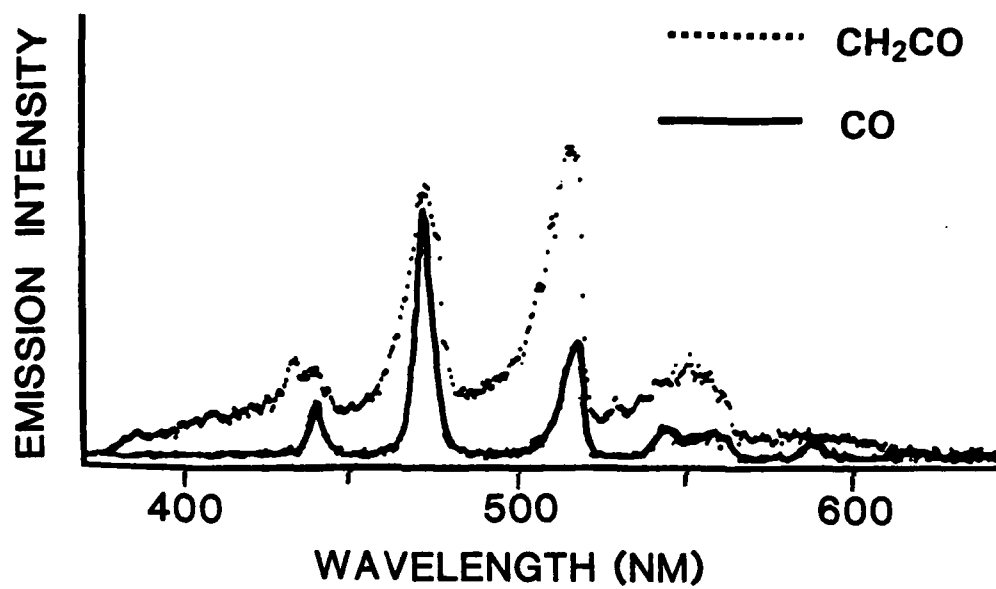


Fig. 2. Low-resolution (2 nm) emission spectra obtained when ketene and carbon monoxide, at 100 torr, are irradiated with individual laser pulses at 266 nm.

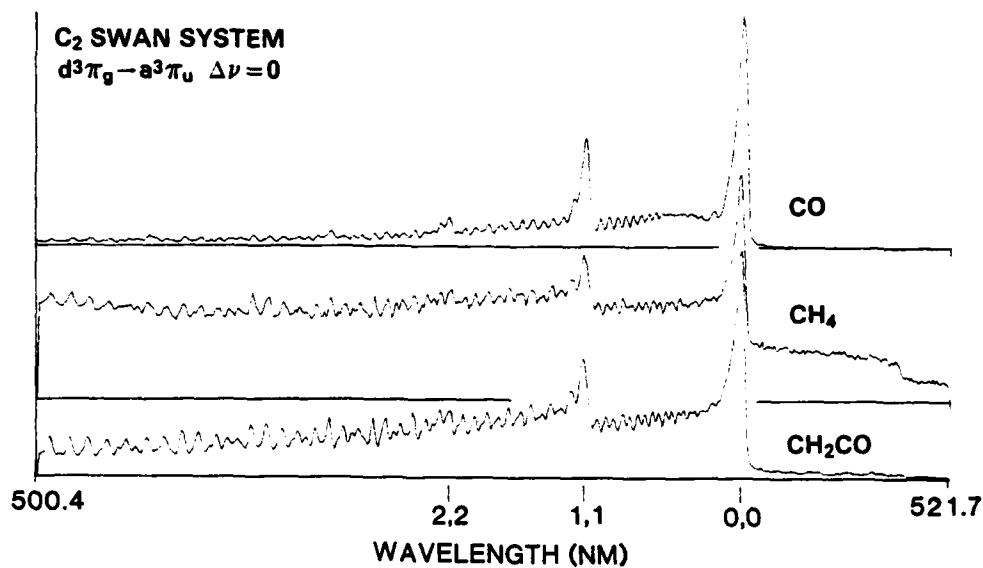


Fig. 3. High-resolution (0.1 nm) spectra of the Swan system emission ( $\Delta\nu = 0$ ) derived from 266 nm irradiation of carbon monoxide, methane, and ketene, at 100 torr. Data are accumulated from 30 laser shots. Note the strong rotational decoration, to the high-energy side of the band heads, for methane and ketene.

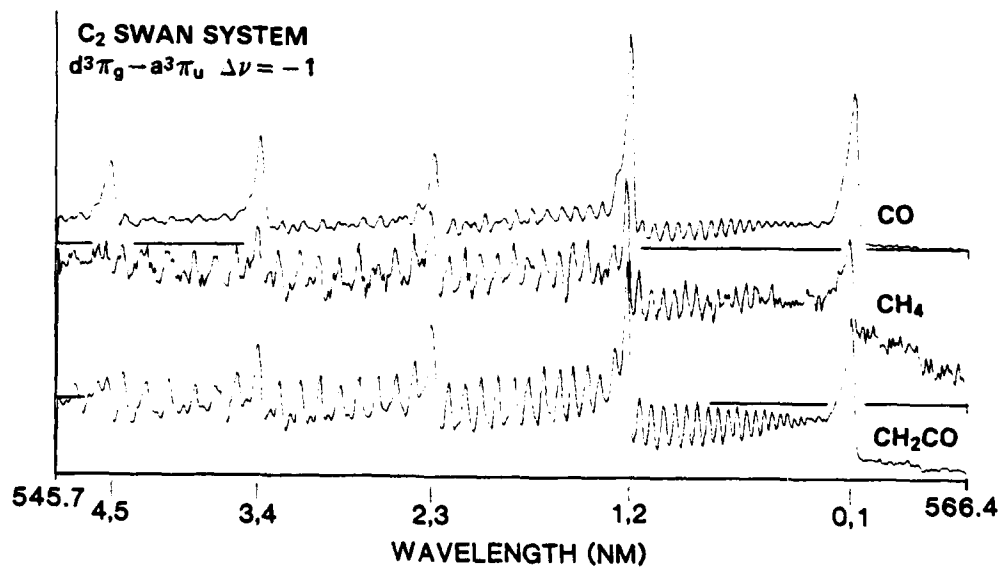


Fig. 4. Spectra of the Swan system emission ( $\Delta\nu = -1$ ). Conditions as in Fig. 3

Figures 5 and 6 compare the regions of Swan  $\Delta v = +1$  and  $\Delta v = +2$  emission from carbon monoxide and ketene. Striking dissimilarities are evident at this resolution. Only in the case of CO are the  $C_2$  "high-pressure" bands (9) observed. These are a consequence of the selective population of an upper vibrational level (generally attributed to  $v' = 6$ ) (9) of the  $d^3\Pi$  state and necessitate distinct formation mechanisms for the  $^8C_2$  produced from carbon monoxide and ketene.

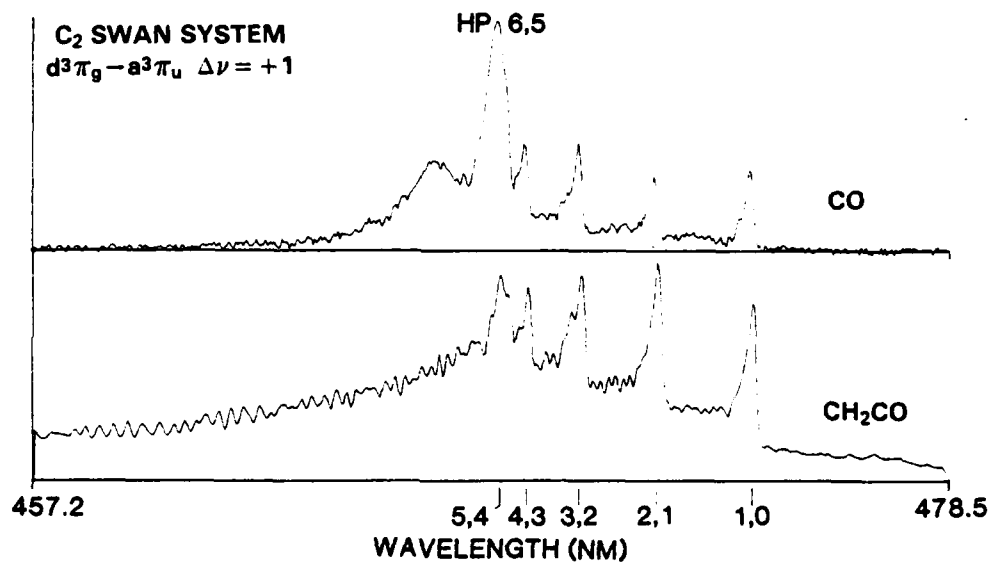


Fig. 5. Spectra of the Swan system emission ( $\Delta v = +1$ ) derived from carbon monoxide and ketene, at 100 torr. Data are accumulated from 30 laser shots. The spectrum from CO also shows the high-pressure 6,5 band.

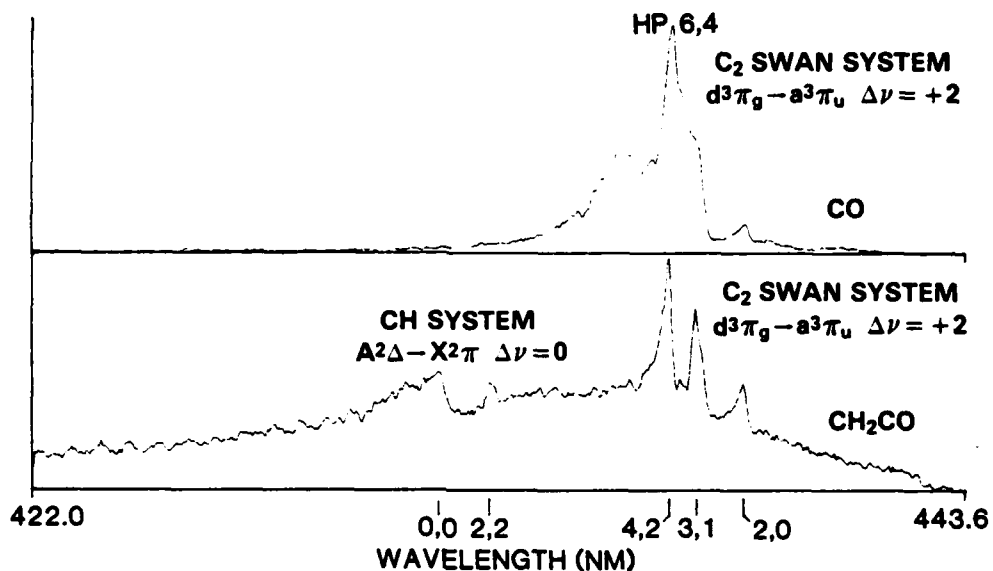
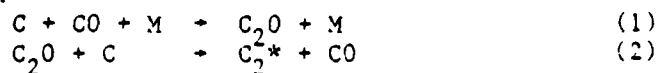


Fig. 6. Spectra of the Swan system emission ( $\Delta\nu = +2$ ). Conditions as in Fig. 5. The spectra also show the high-pressure 6,4 band and CH emissions.

This difference of mechanisms finds further expression in the time-dependent oscilloscope data shown in Fig. 7. Figure 7A shows the risetime-limited formation of the  $d^3\Pi_g$  emissive state (at 516 nm) of  $C_2$  derived from ketene. The risetime is indistinguishable from that of the plasma radiation (upper trace), monitored at 616 nm where Swan emission is negligible. By contrast, no prompt  $C_2$  emission is seen from CO (Fig. 7B) when either the normal or the high-pressure Swan bands are monitored. The oscillogram in Fig. 7B shows only the brief plasma emission, which can be detected throughout the visible region. Over much longer timescales (Fig. 7D), the slow, collisional formation of the  $d^3\Pi_g$  state is observed. An intermolecular pathway leading to the formation of  $C_2$ , like that suggested by Kunz *et al* (10) (see Eqn. (1) and (2)), is consistent with these data:



M represents a third body and \* refers to an unspecified electronic state of  $C_2$ . The highly-specific vibrational population of the

excited state is then rationalized as follows: there is a relaxation of the initial  $C_2$  state to  $b^3\Sigma_g^-$  which crosses  $d^3\Pi_g$  near its sixth vibrational level (11). It has generally been accepted that the high-pressure emission originates from  $v' = 6$ . However, the high-pressure bands lie to the low energy side of the corresponding normal Swan band head, where there are no rotational term differences. For example, the designated 6,5 high-pressure transition is at 468.0 nm while the regular 6,5 Swan band is observed at 466.9 nm ( $8_3, 1_2$ ). On this basis, we infer that the exact crossing between the  $b^3\Sigma_g^-$  must occur below  $v' = 6$ .

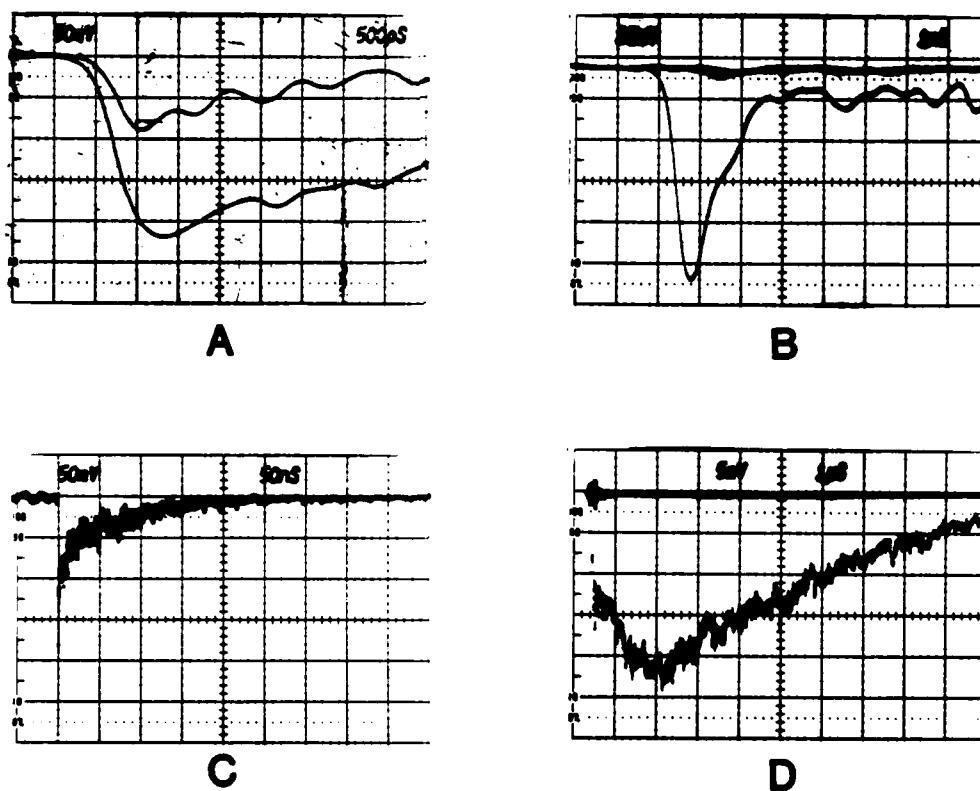


Fig. 7. Oscilloscope traces of the  $C_2$  Swan emission monitored at 516 nm (0,0 transition). **A**: ketene, 100 torr, 500 ps/div. The upper trace shows the plasma radiation at 616 nm and should be reduced by a factor of 2.5 for comparison with the lower trace of  $C_2$  emission. **B**: CO, 100 torr, 1 ns/div. **C**: ketene, 100 torr, 50 ns/div. **D**: CO, 100 torr, 1  $\mu$ s/div.

Since the  $d^3\Pi$  state collision-free lifetime has been determined as ca. 120 ns (3), it is clear that the slower decay in Fig. 7D does not reflect the kinetics of the  $d^3\Pi \rightarrow a^1\Pi$  transition. Evidently we are following the formation and decay steps of an intermediate (consistent with Eqn. (1) and (2)), which become the rate-determining processes for the  $C_2 d^3\Pi$  emission. Figure 7C indicates that the  $C_2 d^3\Pi$  state has a lifetime of ca. 70 ns when produced in 100 torr of ketene. It is likely that the parent molecule and/or other photolysis fragments are involved in quenching steps. For instance, all the hydrogen bearing gases exhibit a strong pressure-broadened emission line at 656.3 nm, assigned to the Balmer  $H_\alpha$  line of atomic hydrogen (Fig. 8).

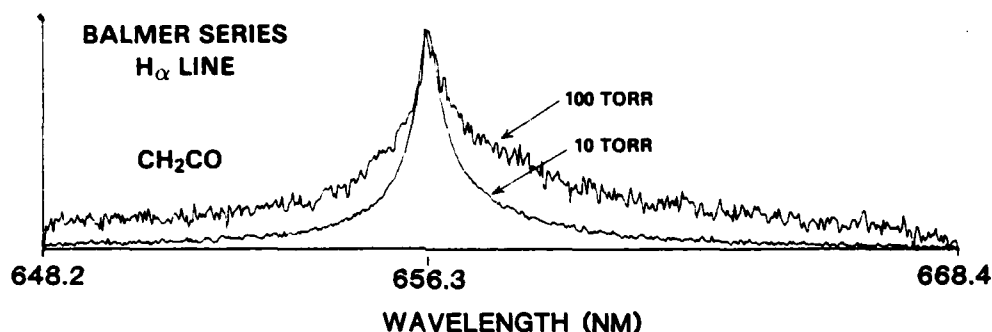


Fig. 8. Spectra of the atomic hydrogen  $H_\alpha$  emission line derived from 266 nm irradiation of ketene. Note the strong pressure-broadening effect.

Returning to Fig. 7A, the  $C_2$  derived from ketene appears with detection-system risetime (as noted in the caption, the contribution of the plasma to the lower trace is minimal). Such prompt  $C_2$  formation suggests a unimolecular mechanism. However, a rapid collisional formation may be envisaged if the reacting fragments are created with substantial kinetic energy. Attempts to observe the formation using a streak camera have proved inconclusive. The spectral resolution required to minimize the prompt background has not allowed sufficient signal to be detected from the  $C_2$  emission. In the case of methane, where  $C_2$  production must be a collisional process, we have nonetheless been unable to follow it kinetically. The plasma radiation dominates the transient signal at 100 torr of methane for several nanoseconds, by which time the  $C_2$  signal is fully developed.

The  $C_2$  emission from methane and ketene show considerable rotational<sup>2</sup> excitation, which implies a non-thermally-equilibrated population of excited  $C_2$  molecules.  $C_2$  emission spectra showing such abnormal rotation are ubiquitous in discharge (13) and laser photolysis (3) studies of simple organic molecules. In an intermolecular mechanism, "off-axis" collisions between fragments would be expected to impart excess rotation to a  $C_2$  product. It is also possible that ketene undergoes unimolecular elimination of hydrogen and oxygen via out-of-plane bending motions, leaving  $C_2$  with rotation. In the case of CO, the  $C_2$  high-pressure system is obtained together with the normal Swan system, both showing the same protracted time development. This now gives temporal as well as spectral inference that  $C_2$  is formed from CO by processes entirely distinct from those in ketene and methane. Consequently, it is not surprising that the emission spectrum exhibits much less rotational fine structure than that derived from ketene and methane.

Weak lines were observed at 410.2 nm and 406.8 nm only when ketene was photolysed. They are attributed to the Deslandres-d'Azambuja singlet  $C_2$  system ( $C^2\Pi_u \rightarrow A^2\Pi_u$ ,  $\Delta v = -1$ ) (8). A weak fluorescence at 431.4 nm (Fig. 6)<sup>8</sup>, observed for ketene and methane is attributed to CH emission ( $A^2\Delta \rightarrow X^2\Pi$ ,  $\Delta v = 0$ ) (8).

The power dependence of the  $C_2$  emission is displayed in Fig. 9. At high input pulse energies, both carbon monoxide and ketene (100 torr) show a near-linear power dependence indicative of a saturation regime. The high-order nature of the excitation process is clearly evident from the steepening of the curves towards lower input energies. Furthermore, focusing of the excitation beam was essential for producing observable emission. Carbon monoxide and methane showed no emission at pressures below 10 torr. Ketene, however, which possesses a single-photon transition at 266 nm ( $\epsilon = 0.5 \text{ mol}^{-1} \text{ cm}^{-1}$ ) (14), exhibited luminescence even at pressures below 1 torr. The streak of visible emission extended somewhat beyond the focal region and had a more diffuse appearance than that observed at higher pressures. The excitation processes may well be different at lower pressures, but the observed luminescent products appear the same.

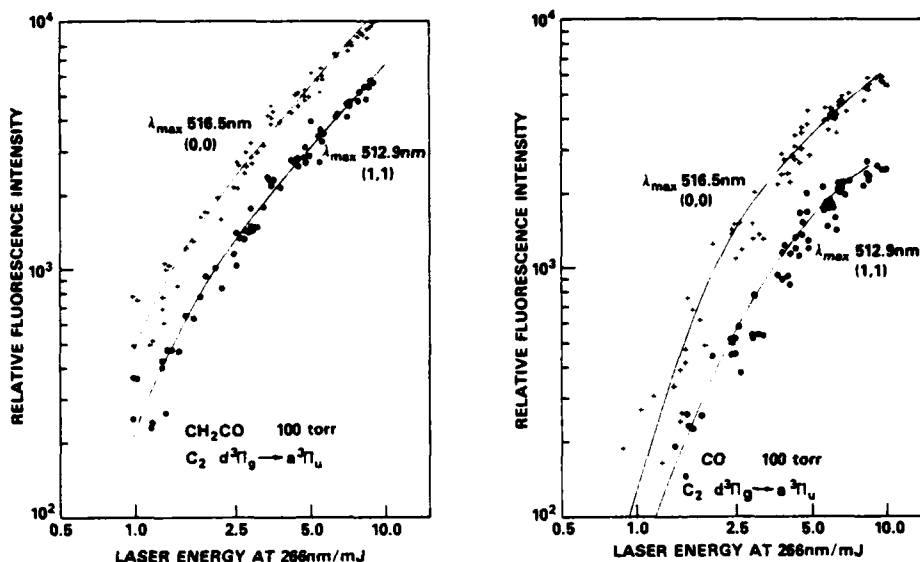


Fig. 9. Dependence of the  $C_2$  Swan emission intensity on input laser pulse energy at 266 nm, from ketene (left) and carbon monoxide (right), at 100 torr.

Figure 10 compares the  $\Delta v = 0$   $C_2$  Swan system observed from 15 torr of nitromethane with that from 10 torr of ketene. The  $C_2$  band is substantially weaker in the case of nitromethane. It shows excess rotational excitation, as for ketene and methane. Furthermore, two new strong emissions were observed with bands heads at 421.6 nm and 388.3 nm (Fig. 10, below). These are assigned to the violet system of CN and arise from  $B^2\Sigma^+ + X^2\Sigma^+$  transitions (8). The  $\Delta v = 0$  transition was also weakly observed in the case of ketene and carbon monoxide, indicating a slight nitrogen impurity.

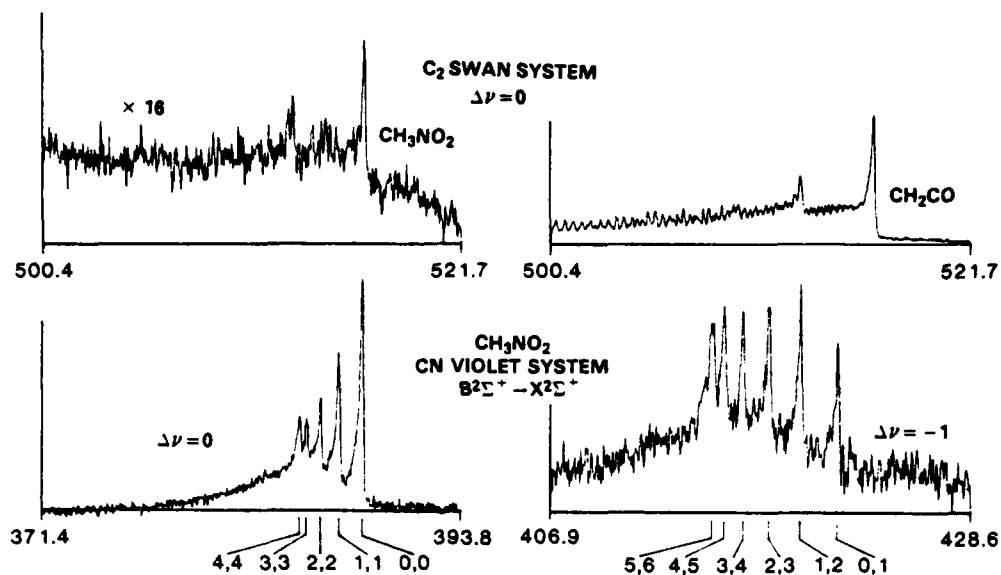


Fig. 10. Above: Spectra of the C<sub>2</sub> Swan emission ( $\Delta\nu = 0$ ) derived from ketene at 10 torr and nitromethane at 15 torr. Note the reduced intensity of the signal from nitromethane. Below: Spectra of the CN violet system emission ( $\Delta\nu = 0$ ,  $\Delta\nu = -1$ ) derived from nitromethane at 15 torr. Data are accumulated from 30 laser shots.

The appearance of the strong CN emission from nitromethane and corresponding decrease in the C<sub>2</sub> emission might indicate that even under these harsh excitation conditions, the C-N bond remains intact. On the other hand, observations from conventional photolysis have been interpreted to support the scission of the C-N bond as the main primary process (15). The CN fragment from nitromethane could be generated unimolecularly, whereas by necessity C<sub>2</sub> is produced collisionally. Experiments are now in progress to follow the time development of the CN emission. In addition, we are examining other nitro-bearing alkanes which could provide an intramolecular C<sub>2</sub> formation pathway as a competing process with CN production.

## SUMMARY

In this work we have extended to the picosecond realm the time definition for laser initiation and interrogation of gas-phase molecular dissociation, with spectral resolution adequate to isolate individual fragment species and indeed to observe rotational structure. We have examined the spectral and temporal characteristics of the dominant emitting fragments,  $C_2$ , CH, CN and H, observed in intense picosecond UV irradiation of ketene, methane, carbon monoxide and nitromethane. The rapid production of the  $C_2$   $d^3\Pi$  state from methane and ketene (limited by the detection system risetime) suggests a similar mechanism of collisional formation, although a unimolecular process can not be ruled out in the case of ketene. Photolysis of CO also yields the  $C_2$   $d^3\Pi$  state, which develops and decays collisionally over several microseconds. Its spectrum exhibits the high-pressure bands and shows much less rotational excitation than that obtained from ketene and methane. It is indicated that a rotationally nonthermalised  $C_2$   $d^3\Pi$  population can be anticipated from precursors bearing  $CH_x$ . For nitromethane, time-resolved studies of the weak  $C_2$  signal and accompanying CN emission should give some insight into the possible dissociative pathways. Future application of this technique to nitro-bearing alkanes and other related compounds may provide important information on reactions through which these molecules communicate in the early phases of rapid decomposition.

## REFERENCES

+ Research supported in part by the Office of Naval Research and the Defense Advanced Research Projects Agency.

1. Chekalin, N.V., Dolzhikov, V.S., Letokhov, V.S., Lokhman, V.N., and Shibanov, A.N.: 1977, *Appl. Phys.* 12, pp 191-195.
2. Lesiecki, M.L., and Guillory, W.A.: 1977, *J. Chem. Phys.* 66, pp 4317-4324.
3. McDonald, J.R., Baronavski, A.P., and Donnelly, V.M.: 1978, *Chem. Phys.* 33, pp 161-170.
4. Filseth, S.V., Hancock, G., Fournier, J., and Meier, K.: 1979, *Chem. Phys. Lett.* 61, pp 288-292.
5. Ronn, A.M.: 1976, *Chem. Phys. Lett.* 42, pp 202-204.
6. Braker, W., and Mossmann, A.L.: 1971, Matheson Gas Data Book.
7. Nutall, R.L., Laufer, A.H., and Kilday, M.V.: 1971, *J. Chem. Thermodyn.* 4, pp 167-174.
8. Pearse, R.W.B., and Gaydon, A.G.: 1965, Identification of Molecular Spectra, Chapman and Hall, London.
9. Herzberg, G.: 1946, *Phys. Rev.* 70, pp 762-764.
10. Kunz, C., Harteck, P., and Dondes, S.: 1967, *J. Chem. Phys.* 46, pp 4157-4158.
11. Read, S.M., and Vanderslice, J.T.: 1962, *J. Chem. Phys.* 36, pp 2366-2369.
12. Johnson, R.C.: 1927, *Phil. Trans. Royal Soc. A.* 266, pp 157-230.
13. Lochte-Holtgreven, W.: 1930, *Z. für Physik.* 64, pp 443-451.
14. Laufer, A.H., and Keller, R.A.: 1971, *J. Am. Chem. Soc.* 93, pp 61-63.
15. Honda, K., Mikuni, H., and Takahasi, M.: 1972, *Bull. Chem. Soc. Japan.* 45, pp 3534-3541.

Brillouin Scattering of Solithane 113 at High Pressure

M. Abebe  
Chemistry Department  
Georgetown University  
Washington, D. C. 20057

P. E. Schoen  
Naval Research Laboratory  
Washington, D.C. 20375

### Abstract

Brillouin spectra from Solithane 113 have been obtained as a function of pressure at 26°C using a Fabry-Perot Interferometer. The modulus was derived from the sound velocity and was found to double as the pressure increased to 2.67 K bar. In addition the modulus was measured as a function of scattering angle in the range 64° to 161.45°. For both the pressure and the angle-dependent data it was found that the moduli were greater at gigahertz frequencies than at one megahertz, indicating frequency dispersion.

Solithane 113 is a polyurethane which has been used as a potting compound for suspending solids and isolating them from thermal and mechanical shock originating in the surrounding environment. Questions have been raised as to its ability to resist cracking when the applied stress has high frequency components, in the gigahertz range. These questions have been prompted by recent work done on crack initiation and propagation theory.<sup>1,2</sup> The theory suggests a possible relation between friability and the frequency spectrum of the elastic modulus of a material. An effort is being made therefore to determine the modulus of Solithane over as broad a frequency range as possible under a variety of experimental conditions. (e.g. vs. temperature and pressure) Here we report initial measurements of the longitudinal modulus,  $M$ , by Brillouin scattering at frequencies of  $\sim 10$  GHz. These experiments were made over a range of frequencies and hydrostatic pressures. An increase in frequency in this range by a factor of 2 produced  $\sim 20\%$  increase in the longitudinal modulus. An increase in hydrostatic pressure from 0-40000 psi resulted in a linear doubling of the modulus. Lower frequency data of Gupta<sup>3</sup> show a similar dependence on pressure, although his moduli at 1 MHz are substantially ( $\sim 25\%$ ) smaller than ours at 10 GHz.

We see therefore that the modulus of Solithane depends significantly on pressure, temperature, and frequency.

The increase of the modulus with frequency and with pressure indicate that the ability of Solithane to insulate included materials from high speed and/or high pressure stress is significantly less than for low frequency, low pressure stress. Brillouin scattering has been used to characterize many polymers.<sup>4</sup> It is a technique in which light scattered at an angle  $\theta$  from traveling thermal sound waves in a material is doppler shifted in frequency

by an amount proportional to the sound velocity of the thermal phonon. An incident beam of light with propagation vector  $k_o = 2\pi/\lambda_o$  where  $\lambda_o$  is the incident wavelength, interacts with thermal phonons in a material of refractive index  $n$ , and is scattered at an angle  $\theta$  with respect to the incident beam. The phonons which couple with the scattered light have a propagation vector  $q = 2\pi/\Lambda$ , where  $\Lambda$  is the sound wavelength.

$$q = 2k_o n \sin(\theta/2) = \frac{4\pi n}{\lambda_o} \sin(\theta/2) \quad (1)$$

The doppler frequency shift of the scattered light is  $f$ , and is related to the sound velocity  $v$  by

$$v = 2\pi f/q \quad (2)$$

Presuming that we are dealing with longitudinal (compressional) sound waves only and assuming that the sound attenuation is small we calculate the real part of the modulus<sup>5</sup> by

$$M' = \rho v^2 \quad (3)$$

where  $\rho$  is the density. The imaginary part of the modulus has the form

$$M'' = \frac{2\rho\Gamma\pi}{q} \quad (4)$$

where  $\Gamma$  is the full width at half maximum height of the Brillouin peaks.

The index of refraction of Solithane as function of pressure is not known. We determined the room pressure index with an Abbe refractometer and extrapolated this value to high pressure with the Clausius-Mossotti relation

$$\rho = c \frac{n^2 - 1}{n^2 + 1} \quad (5)$$

where  $c$  is the proportionality constant.  $n$  is 1.5123 at room pressure and increases to 1.551 and 40000 psi according to this relationship.

### Experimental Details

Solithane 113 pre polymer was manufactured by Thiokol Chemical Corporation and was prepared by California Institute of Technology in the form of transparent sheet with 6 mm thickness.<sup>6</sup> The sample used in these experiments had a 50/50 resin to catalyst mixture. Solithane was cut by razor blade and polished to a smooth finish with emery cloth. For transparency it was inserted in an optical cell with index matching parafin oil. The cell was made large so that the flare spots due to elastic scattering of the laser beam as it entered and exited the cell were distant from the scattering volume. The container was mounted on a rotating optical holder for accurate angular measurement and excitation was achieved by a single frequency 514.5 nm Argon-ion laser.

The experimental arrangement is shown in figure 1. The optical axis of the sample-apertures-Fabry-Perot interferometer-lenses-detector was indicated by a He-Ne laser beam. Alignment was maintained using this reference and the scattering angles were measured by successively reflecting back on themselves from the sample cell entrance window the He-Ne beam and the Ar<sup>+</sup> beam. Corrections to this angle were made for the refractive index of the sample and its index matching liquid. The scattering volume was first imaged on a pinhole to reduce stray light. The light was then re-collimated for the Fabry-Perot and detected by an EMI 9658 phototube with photon counting electronics. Data was stored in a multichannel analyzer.

The Fabry Perot was a Burleigh instrument with 2 inch diameter mirrors, scanned by a home built digital ramp and tuned with an automatic stabilizing servo. This maintained a typical finesse of 40.

For the high pressure experiment solithane was cut to fit the cavity of a 60,000 psi Nova cell. The pressure cell was a 4-window cross design which

permitted easy optical alignment. Pressure was generated by a 40,000 psi Enerpack hand pump and was measured by a 40,000 psi Aminco gauge. The cell was filled with silicon oil for pressure transmission and index matching. We found it necessary to use a separator to isolate the silicon fluid from the colored pump oil. The transparent silicon oil 2) minimized light loss, b) provided index matching, c) did not freeze or deteriorate at the highest working pressure, d) had a convenient viscosity and e) protected the Nova cell from water.

In order to calculate  $\rho v^2$  from equation 3 it was necessary to determine the pressure dependence of the density of solithane 113. An apparatus employing a piston in a capillary tube was designed for the Nova cell such that compression of the sample in the tube could be determined by telescopically observing the motion of the piston.

#### Results and Discussion

Brillouin frequency shifts for solithane were measured for 4 different angles:  $64^\circ$ ,  $90^\circ$ ,  $118.4^\circ$ , and  $161.45^\circ$  at one atmosphere and  $26^\circ\text{C}$ . The longitudinal modulus, calculated from equations 2 and 3, changed nonlinearly from  $6.78 \times 10^5$  psi at  $64^\circ$  to  $7.95 \times 10^5$  psi at  $161.4^\circ$ . These results are plotted in figure 2.

The longitudinal modulus of solithane as a function of pressure is shown in the upper curve of figure 3. Over the 40000 psi range of the experiment the modulus increased linearly to more than double its room pressure value. Similar linear relationships have been seen for other polymers.<sup>8</sup> The 1 MHz data of Gupta is shown in the lower curve. The shift of the modulus to higher values at higher frequencies indicates a significant frequency dispersion in this quantity.

In summary, Brillouin scattering is the only method which easily provides measurements at gigahertz frequencies. We have demonstrated the utility of this technique to the study of the moduli of a commercial polyurethane (Solithane 113) as a function of stress rate and pressure. The twofold increase of the longitudinal modulus with pressure and its sharp increase with frequency indicate that the sample becomes more brittle and glassy in this frequency/pressure regime.

Future work will explore the temperature and pressure behavior of Solithane in the gigahertz frequency regime, with more detailed examination of frequency-temperature-pressure interrelationships. The effect of systematic variations in polymer composition and plasticization will also be determined.

#### Acknowledgements

We acknowledge the support of the Office of Naval Research for some of the work reported here.

We also appreciate permission given by Dr. Y. Gupta to include his data.

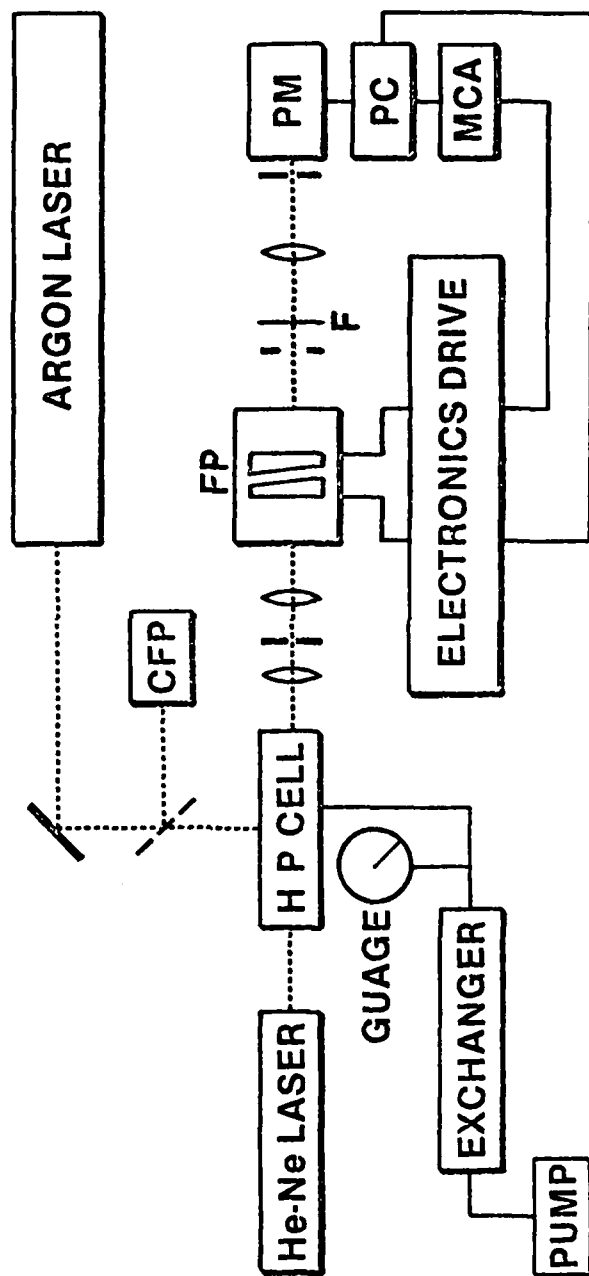


Fig. 1 - Brillouin scattering setup.

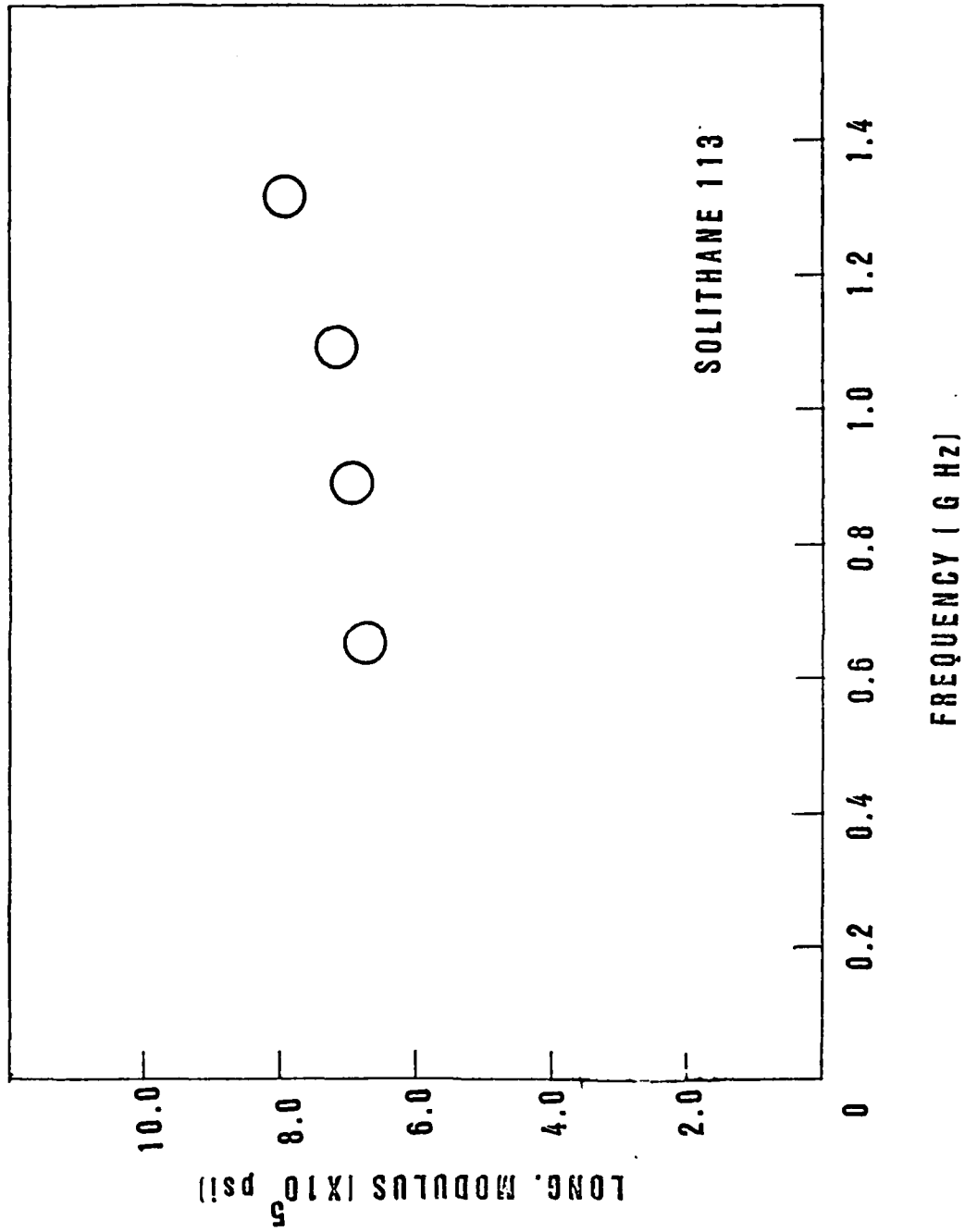
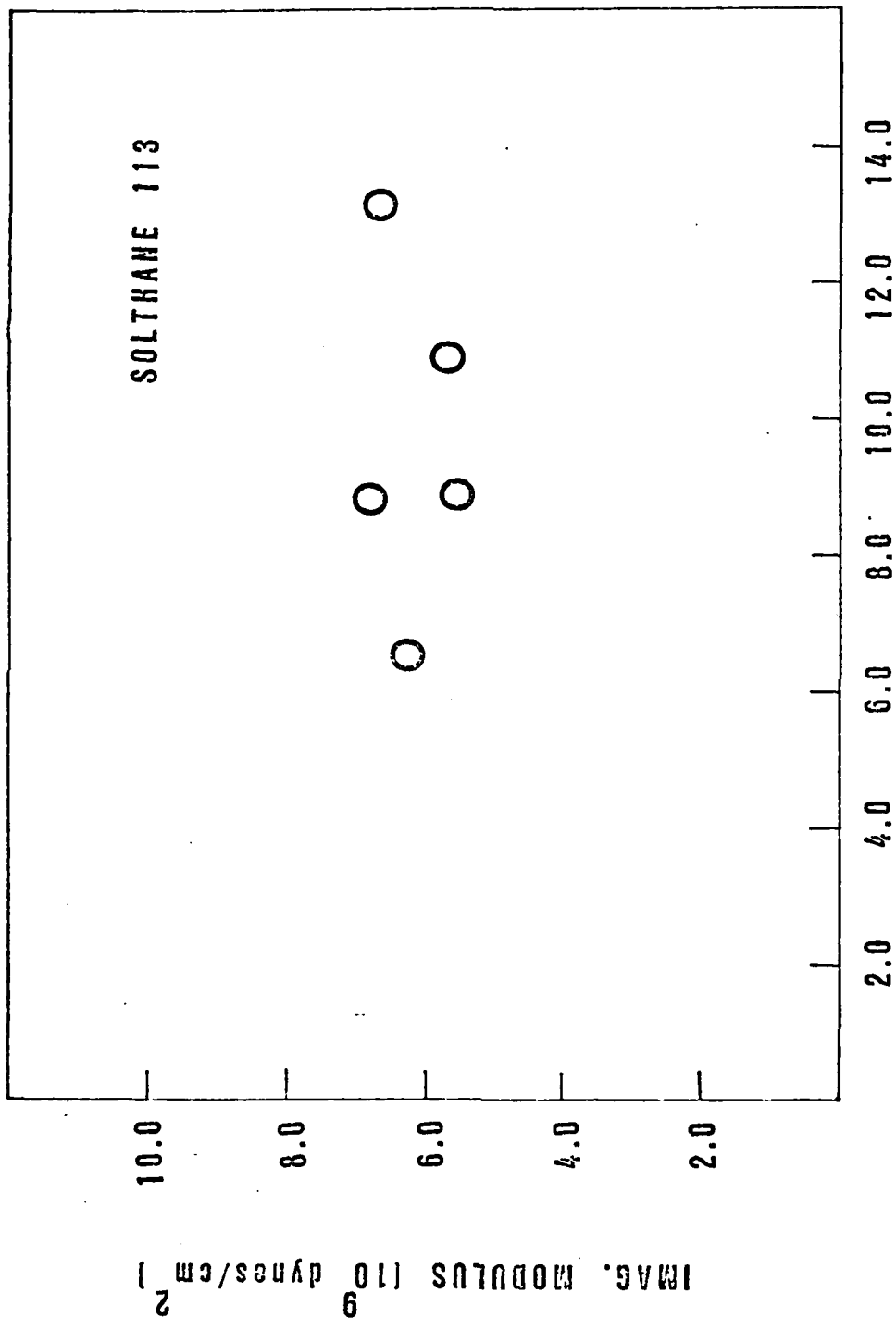
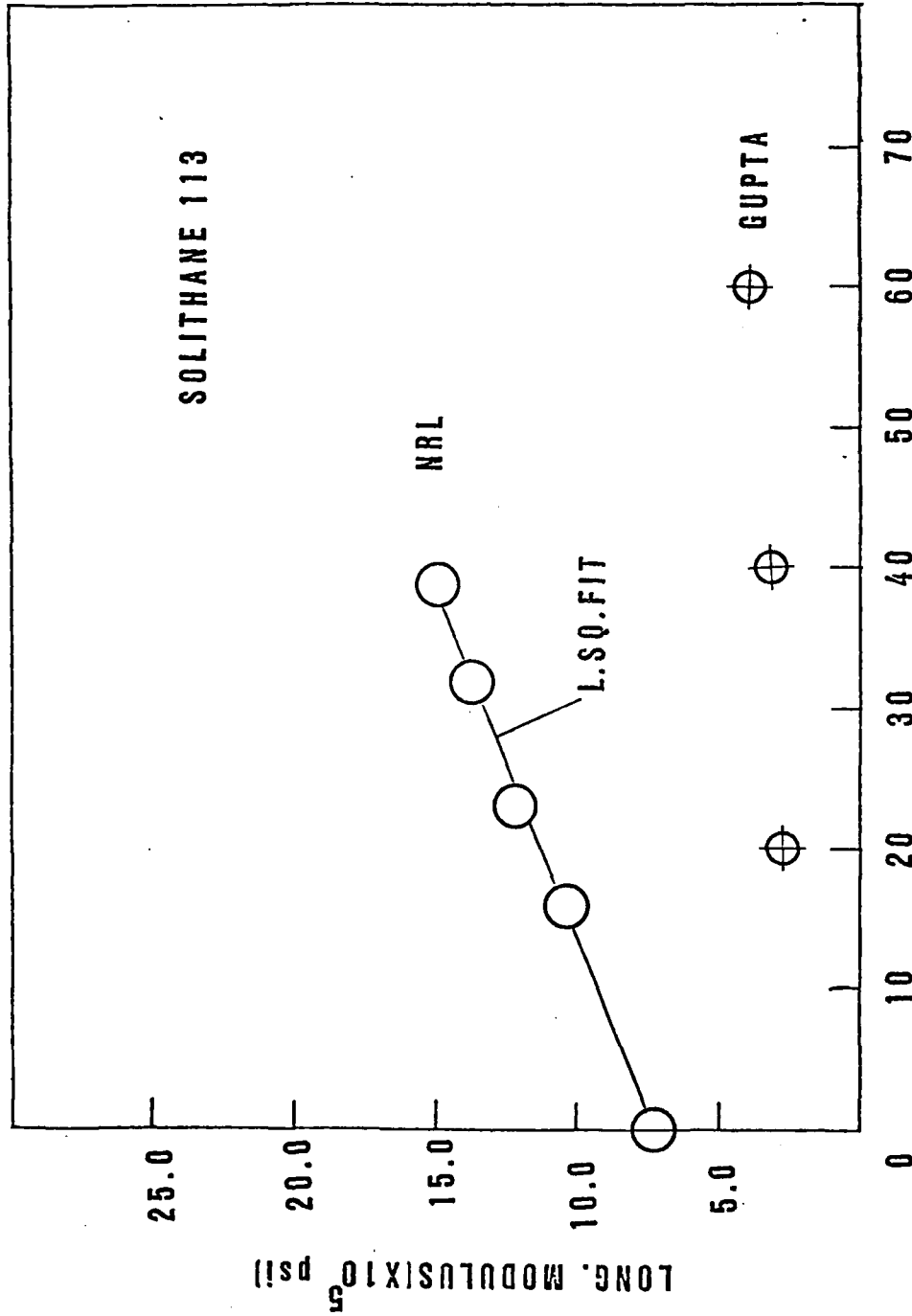


Fig. 2(a) - Longitudinal modulus of Solithane 113 as a function of frequency the real modulus.



FREQUENCY SHIFT ( $\times 10^9$  HZ)

Fig. 2(b) - Longitudinal modulus of Solthane 113 as a function of frequency the imaginary modulus.



PRESSURE (X 10<sup>3</sup> psi)

Fig. 3 - Moduli of Solithane 113 vs pressure. Upper curve:  
real long modulus of Gupta at 1 MHz.

### References

1. R. A. Schöperly, Int. Journal of Fracture 11, 141 (1975).
2. S. R. Swanson, Bulletin of the Seventh Meeting of ICRPG Working Group on Mechanical Behavior, Nov. 1968.
3. Y. Gupta, SRI International, private communication.
4. G. D. Patterson, J. Macromol, Sci.-Phys., 1313, 647 (1977).
5. K. F. Herzfeld and T. A. Litovitz, "Absorption and Dispersion of Ultrasonic Waves" (Academic Press, New York, 1959).
6. W. G. Knauss, "A Cross-linked Polymer Standard Report on Polymer Selection", Polymer Science Report, Materials Science, Calif, Inst. of Tech., Pasadena (1965).
7. M. Abebe and P. E. Schoen, to be published.
8. J. A. Sauer, Polym, Eng. Sci. 17, 150 (1977).

**CPIA PUBLICATION 308**

**DECEMBER 1979**

Reproduction not authorized  
except by specific permission  
from CPIA.

# **16TH JANNAF COMBUSTION MEETING**

**VOLUME II**



**NAVAL POSTGRADUATE SCHOOL**

**Monterey, California**

**September 10-14, 1979**



**CHEMICAL PROPULSION INFORMATION AGENCY**

Operating under Contract N00024-78-C-5384

**THE JOHNS HOPKINS UNIVERSITY · APPLIED PHYSICS LABORATORY · LAUREL, MD.**

Approved for public release; distribution unlimited

APPLICATION OF ADVANCED OPTICAL SPECTROSCOPIC METHODS  
TO ENERGETIC MATERIALS (U)\*

L.S. Goldberg, J.M. Schnur, P.E. Schoen, W.L. Faust, T.R. Royt, S. Wunder,  
and M. Abebe

Naval Research Laboratory  
Washington, D.C. 20375

ABSTRACT

Recent progress at NRL is described on the application of advanced optical spectroscopic methods to the study of energetic materials. Three principal areas of research are highlighted: High-pressure Brillouin and Raman light scattering spectroscopy, and picosecond laser spectroscopy.

INTRODUCTION

The advent of new diagnostic techniques and instrumentation when applied to materials research problems often leads to new insights and deeper understanding of the physical processes under study. This is especially true for the powerful laser spectroscopic methods that have been developed in recent years. The intent of this paper is to describe several areas of research at NRL in which laser light scattering and picosecond spectroscopy are being applied to the study of energetic materials.

Brillouin spectroscopy is being applied to problems associated with binder failure in highly energetic propellant systems. The relationship of molecular properties such as the relationship between high frequency bulk moduli and the propensity for crack propagation in propellant binders is currently under investigation. A collaborative program supported by ONR has been initiated among the California Institute of Technology, the University of Akron, Texas A&M, the Stanford Research Institute and the Naval Research Laboratory in order to study this problem comprehensively, and to provide a possible basis for guidance of future propellant formulation.

Picosecond laser spectroscopy is being applied to the investigation of primary events in the photoinitiation of ultrafast reactions in energetic materials. A collaborative research program has been established with Georgetown University and the Naval Research Laboratory. By utilizing the extreme time resolution afforded by these laser techniques, it is now possible to observe and to follow the time evolution of the earliest product species formed after the initial excitation. Such information can lead directly to a greater understanding of deflagration to detonation transitions (DDT), and can provide insights into the role that additives may play in affecting sensitization of energetic formulations.

The work in these areas has proceeded in several directions and has led

---

\*This research has been supported in part by ONR and NAVSEA.

to some very intriguing findings. Results of these studies are summarized below.

#### BRILLOUIN SPECTROSCOPY STUDIES OF VISCOELASTIC PROPERTIES AS A FUNCTION OF PRESSURE

Polymeric materials are being characterized as a function of pressure using Brillouin spectroscopy to determine the high frequency bulk moduli of these materials. This technique allows the study of the effect of pressure, temperature, sample history, molecular weight, and polymer chemistry upon these high frequency viscoelastic properties. Simultaneously, research groups at Stanford Research Institute and the California Institute of Technology are characterizing these same materials with respect to fracture resulting from the application of stress at ultrafast rates.

It is very likely that the high frequency viscoelastic properties play an important role in the propensity for cracking of solid rocket propellants. Under the severe mechanical and thermal stresses encountered in use, the propellants are subjected to vibrations over a wide frequency spectrum including very high frequencies as well as pressures. The severity of any resultant fracturing can influence whether the propellant will stably burn or, in fact, detonate. Since the maintenance of the structural integrity of a rocket engine over its lifetime requires that the solid propellant also resist creep deformation for periods of years, the time scales of interest for viscoelastic response range from  $10^8$  sec to less than  $10^{-9}$  sec, an enormous span. The Brillouin scattering technique makes possible for the first time the direct measurement of the moduli of real polymeric binders for response times  $\sim 10^{-9}$  sec. This short time regime previously could only be reached by extrapolation or by indirect time-temperature superposition methods.

In Brillouin scattering, laser light of frequency  $\omega_0$  and momentum  $\vec{k}_0$  scatters inelastically from thermally induced density fluctuations (sound-waves) in a sample.<sup>1</sup> The Bragg condition  $q = \frac{4\pi n}{\lambda_0} \sin(\theta/2)$  relates the momentum  $q$  of the sound waves giving rise to scattering into an angular direction  $\theta$ , measured from the incident beam direction. A Fabry-Perot interferometer is used to analyze the collected scattered light into its respective frequencies. From the observed frequency shift  $\Delta\omega$  ( $\sim 10^9$  Hz) of the Brillouin band at a scattering angle  $\theta$ , the velocity of sound in the sample can be calculated as  $v = \Delta\omega/q$ . An independent measurement of sample density  $\rho$  then allows determination of the bulk modulus  $M = \rho v^2$ . For polymeric materials this is the longitudinal modulus, since scattering by shear waves is not observed. Viscosity and relaxation measurements can also be derived from further analysis of the scattering data. Our Brillouin studies of high frequency moduli characterized as a function of pressure are being compared against high-stress-rate relaxation data obtained by the other collaborative groups. To provide a basis for intercomparison of results, the initial-stage experiments are being carried out on a well-characterized polyurethane compound, Solithane 113.

Figure 1 presents Brillouin scattering data of the longitudinal modulus as a function of frequency (stress rate) for Solithane 113 at ambient pressure and temperature. The four data points were obtained at scattering angles of  $\theta = 64^\circ, 90^\circ, 118^\circ, 161^\circ$ , the backscatter geometry corresponding to

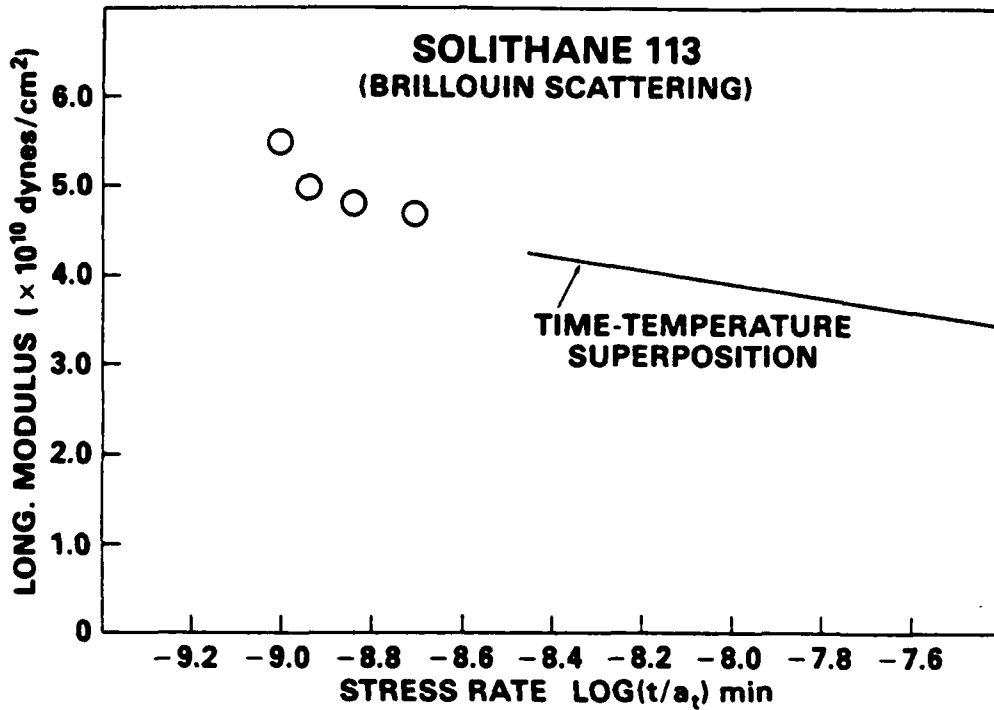


Figure 1. Brillouin scattering determination of high-frequency longitudinal modulus in Solithane 113.

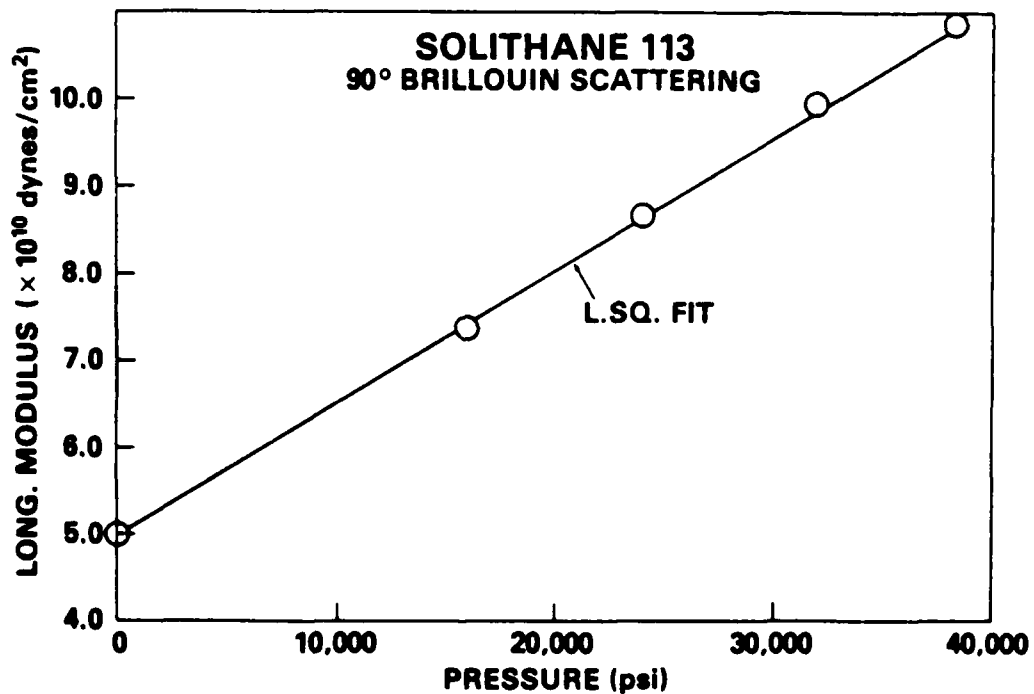


Figure 2. Pressure dependence of longitudinal modulus in Solithane 113.

the highest frequency. These results are seen to scale well with the lower frequency data obtained by Mueller<sup>2</sup> using time-temperature superposition. Figure 2 shows the pressure dependence of the longitudinal modulus of Solithane 113 measured for a 90° scattering geometry. Pressures from ambient up to 2.6 kilobars were applied using a conventional hydrostatic pressure cell. The observed increase of the modulus with pressure indicates that the compressed sample of Solithane 113 under hydrostatic pressure becomes significantly more brittle as pressure is increased.

We have also demonstrated the effectiveness of multipass interferometry in allowing characterization of real polymeric binder systems. Such materials typically are of poor quality, being translucent or having imperfections that scatter light strongly and mask the relevant Brillouin-shifted bands. A single pass interferometer is generally a low contrast instrument in that it has difficulty separating spectral components whose intensities differ by a ratio of more than about  $10^3$ . In the multipass technique the scattered light is sent through the interferometer 3 (or 5) times in succession, thereby improving the contrast ratio to  $10^7$  or better. This contrast improvement has enabled us to obtain the first Brillouin spectrum of the translucent binder material ethyl vinyl acetate, and points the way to a fuller utilization of these techniques.

#### RAMAN SPECTROSCOPY STUDIES OF MOLECULAR PROPERTIES AT HIGH PRESSURE

We are using Raman spectroscopy to study the effects of high pressure upon the microscopic properties of complex molecular systems. In a study directed towards the conformational properties of lubricants and polymers under pressure, we have obtained the Raman spectra of both short and long chain alkane fluids at pressures up to 20 kilobars.<sup>3</sup> The Raman spectrum provides a very sensitive probe of the conformational ordering of the molecules, since the effects of externally applied stress can readily be observed as changes in the vibrational spectrum. To analyse the alkane data, the vibrational frequencies of the different normal modes of the alkanes were first identified through model calculations and by spectroscopic investigations at ambient pressure for the straight chain, all-trans configuration as well as for some of the kinked, gauche conformers. Selected bands were then monitored with applied pressure to ascertain spectral changes that could be attributed to changes in conformational order.

The Raman spectra were measured over a range of 1 to 20 kilobars pressure in a gasketed diamond-anvil cell. Pressures were calibrated in situ using the ruby fluorescence technique. The 752.5 nm line of a Krypton laser was chosen as excitation source, particularly to minimize background fluorescence from the diamond, ruby, and sample. The spectra were recorded using a double monochromator with holographic gratings optimized for the near IR spectral region and a low-noise photomultiplier tube that was sensitive out to 900 nm.

Results from this experiment conclusively show that alkanes (< 16 carbons in the chain) become more globular as pressure is increased. For long chain alkanes (> 40 carbons in the chain) the opposite appears to occur, that they become more rod-like as pressure is increased above 5kb. These unexpected findings for the short alkanes may shed some light upon recent results from viscoelastic studies designed to evaluate the use of

fatty acids as surfactants to minimize friction between metal surfaces. Researchers at both Battelle Laboratories and Rensselaer Polytechnic Institute have reported that these additives unexpectedly increased the wear in some experiments. Some of these findings could be readily interpreted on the basis of the discovery that the short alkane chains become more gauche under applied stress, that is more ball-like.

We are now applying these high-pressure Raman techniques to the study of pressure-catalyzed reactions in alkyl-ammonium, and alkyl-hydroxyl-ammonium nitrate systems. It is possible that these compounds undergo condensation reactions, catalyzed by high pressure, to form azo compounds. This would have a profound effect upon propellant systems designed to use these types of liquid propellants at elevated pressures. We are currently studying the effect of pressure upon these systems utilizing both Raman and Fourier Transform IR techniques in a diamond-anvil cell.

### PICOSECOND LASER PHOTOLYSIS OF ENERGETIC MOLECULES

Picosecond laser spectroscopy techniques are being applied to studies of small molecular fragments, stable or reactive radical species that are emergent as the primary products of unimolecular decomposition of simple photolabile materials. The initial project in this area has been the study of the picosecond photolysis of nitromethane ( $\text{CH}_3\text{NO}_2$ ), the simplest of the nitro explosives.<sup>4</sup> In spite of many years of investigation and numerous experimental approaches, both the qualitative and quantitative aspects of the photo-induced decomposition of nitromethane remain unclear. This disparity has arisen, in part, from the many experimental conditions of temperature, phase, irradiation wavelength, and pulse duration under which the reactions have been conducted. While the earlier studies have suggested various reaction mechanisms, none has involved measurements on a time scale short enough to observe the initial decomposition products.

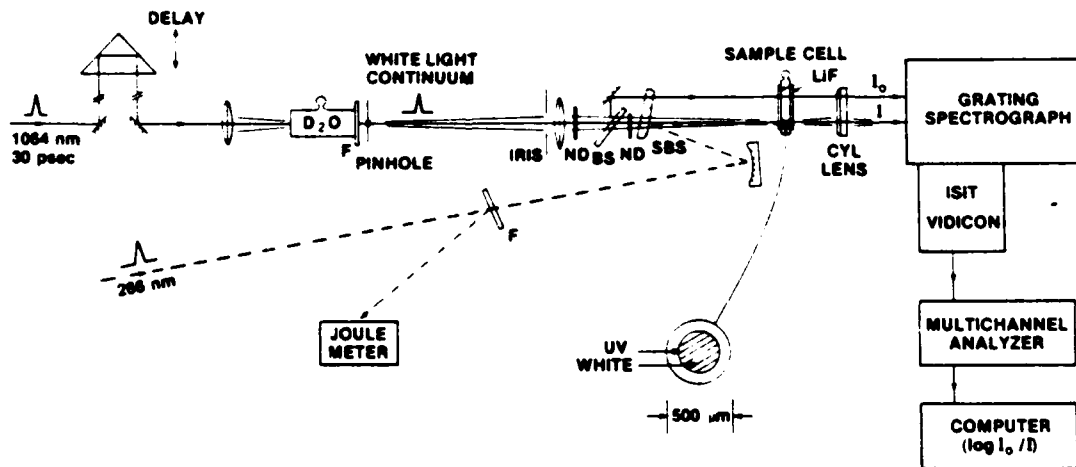


Figure 3. Apparatus for picosecond UV photolysis and dual-beam absorption spectroscopy.

We have constructed a picosecond photolysis and dual-beam transient absorption apparatus (Fig. 3) with the capability to observe spectra of weakly-absorbing transient species. The  $\text{NO}_2$  radical is such an example,

having a broad absorption band extending roughly from 300 to 550 nm with a very low peak cross section of  $\sigma \sim 3 \times 10^{-18} \text{ cm}^2$ . The laser system comprises a flashlamp-pumped, passively modelocked Nd:YAG oscillator, single pulse selector, Nd:YAG preamplifier, 50% beam splitter to provide two independent beam arms, spatial filters, and Nd:YAG final amplifiers for each arm. The amplified 1064 nm pulses are each of 30 picoseconds duration and over 30 millijoules energy. Two stages of frequency doubling in one beam provide a photolysing pulse at 266 nm of up to 10 millijoules energy. The 1064 nm pulse in the second beam arm passes through a variable optical-path delay and is focused into a cell of  $\text{D}_2\text{O}$  to create a white-light continuum pulse for probing. The emergent continuum pulse, also of short duration, is then steered through a 400  $\mu\text{m}$  pinhole just beyond the  $\text{D}_2\text{O}$  cell and is imaged into the liquid sample cell. A beam splitter diverts a replica of the probe beam to impinge on a second spot in the sample for use as reference. Both the UV and probe pulses are made collinear and focused independently into the sample. The spectrum of induced absorption is measured on individual laser shots by dual-beam digital ratiometry using a grating spectrograph, intensified vidicon multichannel recording, and computer data processing.

The measurements were carried out on condensed-phase nitromethane (neat and in solution). A short UV pulse at 266 nm photolysed the molecule through excitation on its first electronic absorption  $n \rightarrow \pi^*$ . The first product species observed was identified by its absorption spectrum as the  $\text{NO}_2$  radical. It was produced with a substantial quantum yield after a protracted delay of several nanoseconds (Fig. 4). This observed delay precludes the excited

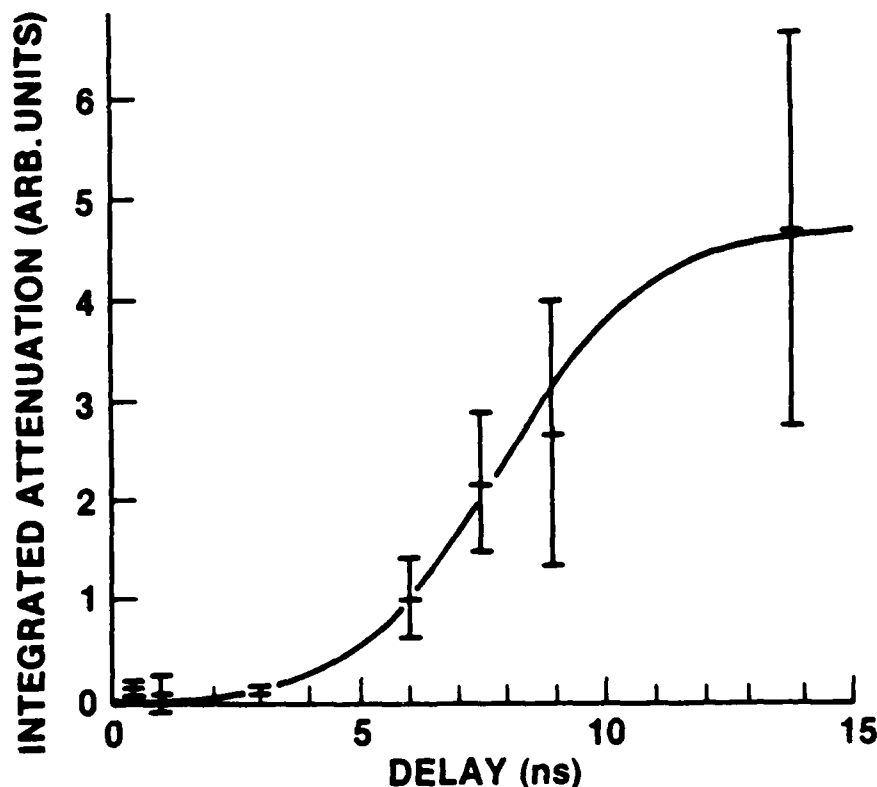


Figure 4. Time development of  $\text{NO}_2$  formation in UV photolysis of  $\text{CH}_3\text{NO}_2$ .

singlet as being the immediate precursor, and suggests possibly a triplet state of nitromethane or an isomer such as the aci form as the initial product of photolysis. The effects of various additives upon the formation kinetics of NO<sub>2</sub> are now being studied. These experiments appear significant in view of the recent reports<sup>5</sup> that small concentrations of ethylamine additives markedly increase the sensitivity to detonation of nitromethane. Finally, we are also currently studying the formation of the highly-reactive methylene molecule in ketene photolysis utilizing similar picosecond spectroscopic techniques. These results will be applied to a study of methylene's role in fast reactions in alkane fuels.

#### SUMMARY

We have discussed several experimental areas in which laser light scattering spectroscopy and picosecond laser spectroscopy are being applied to elucidating information critical to the understanding of energetic materials and their reactions. The potential of these advanced spectroscopic methods in providing a unique microscopic viewpoint of complex physical processes has only begun to be exploited.

#### REFERENCES

1. H. Cummins and P.E. Schoen, Chapter V.1., in Laser Handbook, F. Arecchi and E.O. Schultz-Du Bois, Eds. (North Holland, Amsterdam, 1973).
2. H.K. Mueller, NASA CR-105 392 (N69-35849), (California Institute of Technology, Pasadena, 1969).
3. P.E. Schoen, R.G. Priest, J.P. Sheridan, and J.M. Schnur, Nature **270**, 412 (1977); ibid, J. Chemical Physics, **71**, 317 (1979).
4. W.L. Faust, L.S. Goldberg, T.R. Royt, J.N. Bradford, R.T. Williams, J.M. Schnur, P.G. Stone, and R.G. Weiss, in Chemical Physics 4: Picosecond Phenomena, (Springer-Verlag, New York, 1978).
5. B.N. Kondrikov, G.D. Kozak, V.M. Raikova, and A.V. Starshinov, Doklady Physical Chemistry (translated), **233**, 315 (1977); F.E. Walker, Acta Astronautica **6**, 807 (1979).

# FUNDAMENTALS OF TRIBOLOGY

Proceedings of the International  
Conference on the Fundamentals of  
Tribology

held at  
The Massachusetts Institute of Technology  
Cambridge, Massachusetts  
June 1978

Edited by  
N. P. Suh  
and  
N. Saka

**The MIT Press**  
Cambridge, Massachusetts, and London, England

# APPLICATION OF ADVANCED LIGHT SCATTERING TECHNIQUES TO THE STUDY OF POLYMER PROPERTIES

J. M. Schnur, P. Schoen and S. L. Wunder

## ABSTRACT

*It has been well established that a polymer's propensity to wear is related to its toughness or viscoelastic properties. Unfortunately, the specific variables contributing to a material's 'toughness' are neither well understood nor easily measured. This presentation will discuss the types of relaxation phenomena and relaxation times that are important to the viscoelasticity of a material, their molecular basis, and the various optical techniques available for the characterization of these properties. Specifically the application of Raman, Brillouin, and correlation light scattering techniques to the characterization of solid polymeric materials will be discussed with particular emphasis placed on the relationship between types of information one can obtain from these light scattering experiments and the strength of polymeric materials.*

## INTRODUCTION

Single component polymers can vary in molecular weight, dispersity, crystallinity and morphology, all of which affect material strength and wear. Indeed, a polymer can manifest a range of macroscopic properties (density, tensile strength, etc.) while its chemical composition, molecular weight and molecular weight distribution are kept constant. This is possible because the microscopic properties of molecular conformation and orientation profoundly affect macroscopic properties. Thus if we are to understand fully the mechanisms of strength and wear in polymers we must be able to probe them on the molecular level.

The response of a polymeric material is dependent on the frequency of the applied load, making it important in polymer characterization to measure material properties over a wide frequency range. Information on time scales not measurable by available techniques is typically obtained by making use of the time/temperature superposition principle (which implies equivalence of frequency and temperature for some systems); dynamical mechanical measurements made over a limited frequency range at a series of temperatures are converted to plots spanning a wide range of frequencies at a single temperature. It is clearly preferable to be able to measure a material's response in real time, thereby avoiding the assumptions inherent in time-

temperature superposition. Recently, progress has been made towards this goal with the application of light scattering techniques to the problem of polymer characterization.

Information about the internal dynamics of a polymer is obtained from the frequency changes light undergoes when it is scattered. A single frequency  $\nu_0$  of light from a laser strikes a sample and is scattered with a new frequency or frequencies. The change in frequency  $\Delta\nu$  is characteristic of some process in the sample. Thus  $\Delta\nu$  may be a doppler shift caused by reflection of the light from a moving particle, or else it may be the frequency of a sound wave in the sample or of a molecular vibration.

Light scattering can be divided under the broad subheadings of correlation, Brillouin, and Raman scattering according to the ranges of the frequency shifts involved. Figure 1 indicates the frequency ranges spanned and the molecular processes expected to occur within those frequency domains.

Correlation spectroscopy deals with the lowest frequencies detectable by the light scattering technique. The name, correlation, refers to the electronic technique of processing the detected optical signal. The resurgent correlation function can be fourier transformed to give its frequency spectrum (the range is roughly 0.1 Hz to 1 MHz). As indicated in Figure 1 this range corresponds to the slow, diffusive motions of large polymer chains and chain segments. The technique is used to observe the Brownian motion and rotation of polymer molecules in solution (light scattered from the moving particles is doppler shifted) and slow relaxations in solids near the glass transition,  $T_g$ . It also can be used to determine thermal conductivity, viscosity, and other transport properties through the local density fluctuations these processes cause.

At higher frequencies interferometric means can be used to measure frequency shifts. The lower frequency limit is about 1-10 MHz (depending on laser frequency stability). The upper limit is usually about 100 MHz although there is no reason in principle why one could not work at frequencies several orders higher than this. Figure 1 shows that this range deals mainly with Brillouin scattering, i.e. scattering due to sound waves. The technique determines the elastic moduli (or in fluids, the compressibilities) governing sound propagation. In turn these moduli depend on high frequency collision-induced relaxations. In fluids the tumbling of smaller molecules, depending upon high frequency viscosity, falls into this range, as does the vibrational motion of small molecules and molecular segments in crystals and plastic crystals.

In Raman scattering, dealing with the highest frequency shifts,  $10^{10}$  to  $10^{14}$  Hz, spectral information is measured by diffraction grating. In this regime, light scattering is a true molecular probe, as shown in Figure 1, revealing the motions of atoms relative to each other, and sensitive to crystallinity and molecular conformation. In the lower end of this region are found the so-called longitudinal 'acoustic' modes (LAM's) whose frequencies are inversely proportional to the length of straight molecular chain segments in polymers. There is currently much interest in LAM's because of the information they yield about molecular conformations.

Optical measurements have the additional useful properties: (1) we can see the part of the sample that is being probed by the light beam, (2) the beam can be focused to a spot as small as a few microns if desired for looking at very small samples or regions of samples, and (3) light scattering can be done remotely on samples located inside pressure cells, tempera-

ACOUSTIC VIBRATIONS  
ELASTIC MODULI  
COLLISIONAL RELAXATION

MOLECULAR ROTATION/LIBRATION

TRANSPORT PROPERTIES  
DIFFUSION  
THERMAL CONDUCTIVITY  
VISCOSITY

LARGE CHAIN  
MOLECULAR SEGMENTS  
TORSION/TRANSLATION

MOLECULAR  
STRUCTURE:  
INTRA-MOLECULAR  
VIBRATIONS

CRYSTAL STRUCTURE:  
LATTICE VIBRATIONS  
"LAM"

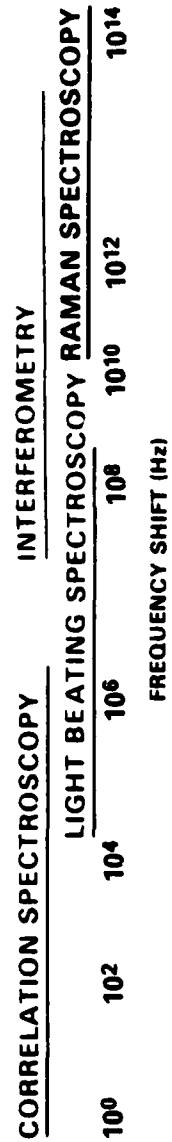


Fig. 1. Range of frequency shifts encountered in correlation, Brillouin and Raman spectroscopy and the excitation frequencies in various samples which these techniques may be used to measure.

ture baths, or even at great distances such as the tops of factory smokestacks...

The typical sample has many processes occurring within it which cause light scattering so that there is usually a great deal of information available in a spectrum. Interpretation of this information is the chief task of the spectroscopist. Light scattering is used in combination with X-ray diffraction, neutron scattering, deuteration and other isotopic substitution, chemical labeling and substitution, computer modeling and other techniques to classify and identify spectral features seen in different circumstances in different compounds and classes of compounds. Since the discipline of light scattering is mature, a considerable library of information is now available that can be brought to bear upon new problems. The art of sorting out the details of a spectrum, drawing upon this pool of techniques and past work, has advanced considerably. Today there is the potential of utilizing this experience in the pursuit of a fuller understanding of the observed macroscopic properties of polymeric materials.

#### CORRELATION SPECTROSCOPY

The correlation technique<sup>(1,2)</sup> has been used in light scattering for about fifteen years. The technique has had broad application to problems both biological and physical. Among the first uses were investigations of transport properties of fluids near their critical points<sup>(2-4)</sup>, and of the diffusive motions (translational and rotational) of large macromolecules and viruses for the purpose of determining their sizes and shapes.<sup>(1,3,5)</sup> Another type of experiment has been measuring chemical reaction rate constants by observing fluctuations in the fluorescence of reacting species.<sup>(6)</sup> Liquid crystal dynamics and viscoelastic constants have also been observed.<sup>(1)</sup>

Correlation spectroscopy has been used to measure doppler shifts caused by blood flow in the arteries of living animals<sup>(7)</sup>, to determine particle velocities in wind tunnels and jets<sup>(8)</sup>, and to obtain the viscosities of lubricants by measuring the velocity with which a slug falls through the viscous liquid.<sup>(9)</sup> This last technique is quite new and extends the range of viscosities which can be measured by the falling slug method by one or two orders of magnitude (to about  $10^6$  poise), while reducing the time required for the measurement from hours to minutes. To determine still higher viscosities (up to  $10^{12}$  poise) correlation measurement of the distribution of fluid structural relaxation times (the diffusive "Mountain mode") has been shown to give good results in lubricants subjected to very high pressures and characterizes the dynamic viscosity over a range of frequencies.<sup>(10)</sup> Figure 2 shows the distribution of relaxation times for a pair of lubricants whose short time lubricating abilities differ sharply because of the difference in their short time relaxation behavior.

A substantial amount of the work done by correlation spectroscopy has been in the area of determining relaxation times for polymer chains in dilute solution.<sup>(11)</sup> The relaxation times for depolarized light scattered in the forward direction from polymer molecules were measured and extrapolated to infinite dilution. The relaxation times obtained were compared initially to the predictions of the Rouse-Zimm model and found in general to disagree, except for the longest wavelength internal motions.<sup>(12)</sup> It was found, again contrary to prediction, that the local diffusive relaxation of fluctuations in position of small polymer segments in a large random coil

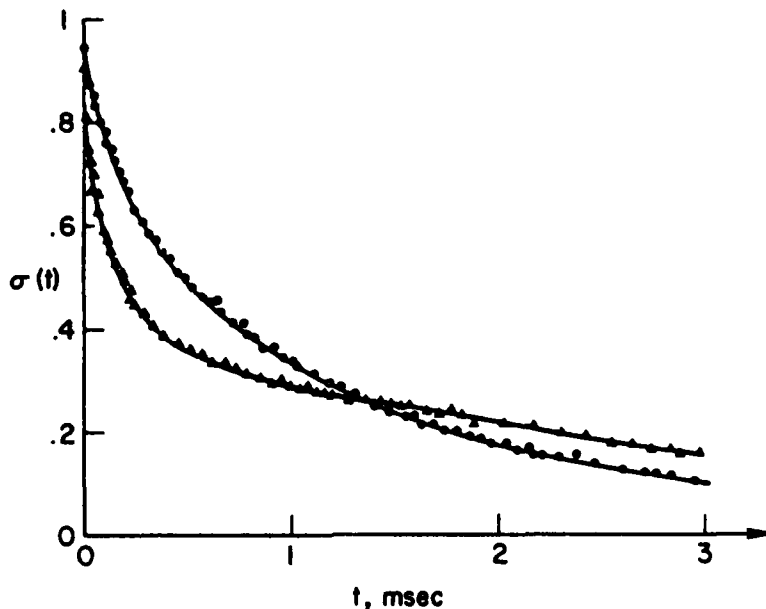


Fig. 2.—Correlation functions  $\sigma(t)$  for a polyphenyl ether (1) at 1.2 kbar pressure and for a short chain methyl phenyl siloxane (2) at 2.1 kbar. The two curves illustrate relaxation functions for liquids which have the same low frequency, long time scale viscosity. The latter polymer will quickly relax a suddenly applied stress whereas the former will not.

(Permission of C. Montrose (ref. 10) to reproduce this figure is gratefully acknowledged.)

resembled that of independent small molecules. Recent measurements by Caroline and Jones (13) show good agreement with an improved theoretical model.

All of the above cases have involved fluids or suspensions of particles in fluids. Use of a correlator with solid materials is rare because of the strong stray light scattering from such samples. However, recently the method has been used to measure low frequency motions in PMMA (14,15) as a function of temperature near the glass transition. Two relaxation times were observed of order .1 sec and .01 sec. The shorter time changed as a function of temperature below  $T_g$ . Its activation energy was found to be lower than that assigned to the side-chain molecular reorientations from dielectric and NMR measurements. The internal motion observed from the correlation spectroscopy experiments was thus thought to arise from a coupling of this side-chain motion with the low activation energy process of torsional oscillations of the chain segments about their equilibrium positions. The longer relaxation time observed was temperature insensitive below  $T_g$  but merged with the backbone main chain relaxation at  $T_g$ . The measurements of this internal relaxation mode above  $T_g$  in the bulk phase by correlation spectroscopy agreed reasonably well with those obtained by mechanical and dielectric measurements. The relaxation below  $T_g$ , which has

not been observed by other techniques, was thought to represent a rearrangement of free volume or of "configurational entropy."

#### BRILLOUIN SPECTROSCOPY

Brillouin spectroscopy<sup>(16)</sup> is light scattering caused by high frequency (10 MHz to 100 GHz) sound - i.e. random thermal oscillations which are always present in a sample with a non-zero temperature. The mechanism of scattering resembles that of Bragg X-ray diffraction, with a sound wave causing diffraction instead of crystal layers. As with Bragg scattering, the scattering angle determines the sound wavelength observed, but since the sound wave is moving, the scattered light is doppler shifted in frequency relative to the incident frequency. From the doppler frequency shift one can determine the velocity of sound. The absorption of sound is determined from frequency broadening of the scattered light. In turn one can then find the viscoelastic moduli of the sample and related transport properties, such as viscosity, thermal conductivity, and diffusion coefficients.<sup>(1,17)</sup> We note here that processes at such fast rates - on the nanosecond time scale - are difficult or impossible to obtain by ultrasonic methods and that X-ray and neutron techniques which do go to such frequencies are considerably less accurate and more difficult, expensive, and damage the sample.

A very large amount of work has been done on a wide variety of fluids and solids to determine their moduli, transport properties, and relaxation times. We will restrict our attention to a few examples chosen from the field of polymers. Energy in such systems is exchanged between molecular internal vibrations and external translational motions.<sup>(18)</sup> Processes which occur faster than such energy exchange encounter considerably different compressibilities and viscosities, for instance, than slower processes do.<sup>(1,19)</sup>

Paraffin oils have been examined in depolarized Brillouin scattering.<sup>(20)</sup> The tumbling of such chain molecules produces a spectral line whose width is related to viscosity. Linewidths were measured as a function of chain length and temperature and the values of the rotational relaxation time were compared with those obtained from flow birefringence. The values were similar but not identical, indicating a possible change in paraffin chain flexibility with longer chains. The relaxation times exhibited an Arrhenius temperature dependence and yielded rate-activation energies which had a chain length dependence.

Brillouin spectra have been obtained for poly (dimethyl siloxane) (PDMS) of molecular weight  $7.7 \times 10^4$  and reveal four relaxation peaks in the hypersonic absorption as a function of temperature.<sup>(21)</sup> This data with microwave and dielectric relaxation times show Arrhenius type behavior for higher temperatures and WLF behavior below, with a sharp break at  $\sim 180^\circ\text{K}$ . The authors suggest this to be the Debye temperature of

The amorphous polymer poly (methyl acrylate) (PMA) appears to be one of the few solids in which a frequency dependent hypersonic relaxation has been observed.<sup>(22)</sup> Frequency dispersion in solid polymers often occurs at considerably lower frequencies than are encountered in Brillouin scattering so that the parameters obtained, such as the velocity, are generally the infinite frequency values. For PMA the glass temperature is  $\sim 60^\circ\text{C}$ . Relaxation is observed at temperatures above  $85^\circ\text{C}$  in both the hypersonic velocity and attenuation, and the size of the relaxation phenomenon is frequency dependent. Using a single relaxation time theory the infinite frequency velocity

and the relaxation time were determined. The value of the activation energy (7 Kcal/mole) suggests the relaxation is of the  $\beta$  type (side chain).

The Landau Placzek (LP) ratio - the ratio of the elastically scattered (zero frequency shift) light intensity to the Brillouin intensity - is often used as a probe of solid polymer behavior under stress. The Brillouin intensity should be relatively constant, as it is an intrinsic property of the material. The elastic scattering on the other hand is sensitive to impurities, domain boundaries, strains, inclusions, etc. Mitchell and Guillet<sup>(23)</sup> and Coakley et al.<sup>(24)</sup> have studied the effects of annealing upon the LP ratio and they have suggested that as the temperature of a sample is dropped the naturally occurring fluctuations in the material are "frozen" in below the glass temperature. The LP ratio then is related to the amount of strain energy stored in the glass.

One of the difficulties of Brillouin scattering in amorphous solids is "contrast," the ability of the spectrometer to distinguish the Brillouin lines, which are weak, from the nearby elastic scattering peak, which is very strong. In recent years considerable progress has been made in improving contrast by the technique of multipassing<sup>(25)</sup> which increases contrast by many orders of magnitude. Dil et al.<sup>(26)</sup> and, very recently, Sandercock<sup>(27)</sup> have reported use of 5 and 7 pass systems to observe Brillouin scattering in metal surfaces. Since the penetration depth of light into a metal surface is small, the technique yields elastic moduli for the region within a few hundred angstroms of the surface. Other phenomena such as the propagation of Lamm acoustic waves in thick films also can be observed.<sup>(27)</sup>

#### RAMAN SCATTERING

In the Raman scattering process<sup>(28,29)</sup> the motion of an atom relative to its neighbors in a molecule or lattice, causes fluctuations in the atomic or molecular polarizability. Since the first observation of the effect almost 50 years ago Raman spectroscopists have used a variety of techniques to determine the nature of the molecular motions which give rise to the Raman spectral lines. This has involved the use of infrared spectroscopy, crystallography, symmetry, substitution of isotopes of different masses onto molecules, and calculations using computer models of molecules and molecular force fields.

One body of work of particular interest in the polymer field has been the application of Raman spectroscopy to the study of crystalline polymer morphology. Many polymers crystallize by folding their long chains into short segments which lie side by side like stacks of soda straws or sheaves of wheat, forming lamellae. The frequency shift of one of the bands of the Raman spectrum, the LAM, is a function of the lamellar thickness. Initial work was done on polyethylene and the n-paraffins.<sup>(30,31)</sup> The latter were used to determine the proportionality constant between the Raman frequency shift and the inverse of the straight chain length as a function of the number of carbon atoms. Frequency shifts obtained from polyethylene samples having lamellar morphology could then be correlated with lamellar thickness assuming that the Raman band corresponded to chain segments whose fold length was that of a similar n-paraffin.<sup>(31)</sup> For polyethylene single crystals where the tilt angle between the chains and the lamellar surface could be determined independently, lamellar thicknesses determined by the Raman method agreed fairly well with those obtained using small angle X-ray scattering (SAXS).<sup>(32)</sup>

Comparison has been more difficult for samples crystallized from the melt, since the tilt angle is generally unknown. Recent work has focused on the effects of the gauche (twisted) segments in the amorphous loop region<sup>(33)</sup>, and of conformational<sup>(34)</sup> and mass defects<sup>(35)</sup> on the frequency of the LAM. This data has yielded information on the nature of the chain fold in polyethylene.

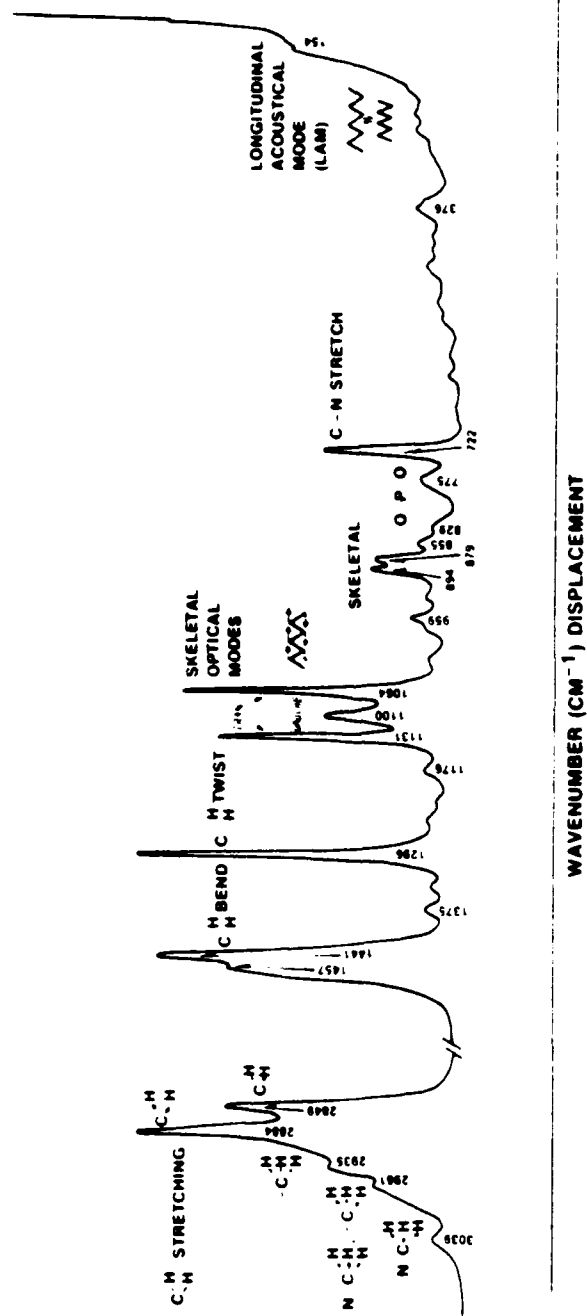
Despite initial difficulty, LAM's have now been observed in the helical polymers polyethylene oxide<sup>(36)</sup>, isotactic polypropylene<sup>(37,38)</sup>, polyoxymethylene<sup>(38)</sup> and in the copolymers (random) tetrafluorethylene - hexafluoropropylene<sup>(39)</sup> and (block) polyethylene oxide - polypropyleneoxide<sup>(40)</sup>, making it possible to use this Raman band in the study of the crystallization and structure of polymer lamellae. It should be noted that the advantage of the Raman scattering technique is that it does not depend<sup>(33)</sup> on the regularity of the lamellar stacking as is necessary for SAXS. This has permitted the observation of double lamellar populations.<sup>(32)</sup>

If the polymer chain is regarded as a uniform rod the proportionality constant between the LAM frequency and the inverse of the chain length is the sound velocity along the rod,  $v = (E/\rho)^{1/2}$ , where  $E$  is Young's modulus and  $\rho$  is the density. Thus, if an estimate of the tilt angle in the lamellar crystal is made, SAXS long period measurements can be combined with Raman frequency shifts to determine the ultimate Young's modulus of a polymer chain. Reports thus far<sup>(38,39)</sup> indicate that estimates made in this way agree with those determined from inelastic neutron scattering, but are substantially larger than those determined from wide angle X-ray scattering.

One particular class of problem which has received a great deal of theoretical attention for the past 30 years or so has been the mode structure of long chain molecules of the polyethylene type.<sup>(42,42)</sup> Considerable progress has been made in this effort and, of particular interest to us, not only have the normal modes of the ideal straight chain been identified but also the effects upon the spectra of chain kinking have begun to be understood. In addition to the LAM's which give information on the length of straight segments between kinks, spectral features have been identified (see Figure 3) which reveal the relative number of gauche and trans bonds (the "optical skeletal" bands)<sup>(43)</sup>, and the ordering of chains and chain segments relative to each other (the "methylene stretching" bands<sup>(44)</sup> and crystal field splitting<sup>(45)</sup>). These bands have been used to investigate the effects of annealing on polymer lamellae thicknesses<sup>(46)</sup>, the relative elastic moduli of crystalline and amorphous polymers<sup>(47)</sup>, the effects upon chain order in model biological membrane chain molecules caused by phase changes and other perturbations<sup>(48)</sup>, the effect of high pressure upon polymer structure and crystallinity<sup>(49)</sup>, and the effect of high pressure upon chain kinking in the liquid alkanes.<sup>(50)</sup> In the latter case it has been seen that high pressure (up to 20 kbar) causes short chain alkanes (neptane, octane) to kink up and longer chains (polyethylene) to straighten out to the "super extended" chain phase. Work of this nature is continuing now to try to determine the relation between lubricant chain conformation and "lubricity," polymer structure and strength, and the influence upon these properties of perturbations such as temperature, pressure, chain length and dispersity, sample history, etc.

#### CONCLUSION

We have discussed briefly correlation, Brillouin, and Raman spectroscopies and have attempted to demonstrate in a general way their use and



**RAMAN SPECTRUM OF DIPALMITOYL PHOSPHATIDYL CHOLINE  
(EXCITATION SOURCE: KR LASER AT 647 nm)**

Fig. 3. Raman spectrum of the model biological membrane molecule, dipalmitoyl phosphatidyl choline, which shows many of the features typical of paraffin and polyethylene molecules. Each spectral band is labeled with the type of atomic motion causing it and the numbers give the frequency shifts in wavenumbers. (1 wavenumber =  $1 \times 10^{10}$  Hz). The LAM at 154 wavenumbers is fairly weak in this sample whereas in polyethylene and the n-paraffins it is quite strong.

range of applicability. We have tried to show some of their unique abilities while at the same time emphasizing the need to employ them in concert with other spectroscopies and mathematical modeling techniques. We believe that light scattering is unusual and exciting because it is both new and old; new in the sense of new and dramatically improved instrumentation and lengthening list of materials and fields in which it is finding use, and old in the sense of being a mature science with a great store of information and technology available to help with experimentation and interpretation.

#### ACKNOWLEDGEMENT

We gratefully acknowledge the support of the Office of Naval Research for some of the work reported herein.

#### REFERENCES

1. Cummins, H.Z. and Pike, E.R., eds., "Photon Correlation and Light Beating Spectroscopy," NATO Advanced Study Institute, Capri, Italy, 1978; also Plenum Press, New York, 1974.
2. Benedek, G.B., in "Polarisation, Matière et Rayonnement: Livre de Jubilé en l'honneur du Professeur A. Kastler," edited by the French Physical Society, Presses Universitaires de France, Paris, 1969.
3. Cummins, H.Z. and Swinney, H.L., *Progress in Optics*, Vol. 8, 1970, p. 133.
4. Chu, B., "Laser Light Scattering," Academic Press, New York, 1974.
5. Cummins, H.Z., Carlson, P.D., Herbert, J.J. and Woods, G., *Biophysical Journal*, Vol. 9, 1969, p. 518.
6. Elson, E.L. and Maude, D., *Biopolymers*, Vol. 13, 1974, p. 1; and Maude, D. and Elson, E.L., *Biopolymers*, Vol. 13, 1974, p. 29.
7. Riva, C., et al., *Investigative Ophthalmology*, Vol. 11, 1972, p. 936.
8. Birch, A.D., Brown, D.R., Thomas, J.R. and Pike, E.R., *Journal of Physics D: Applied Physics*, Vol. 6, L71, 1973.
9. Jackson, D.A. and Bedborough, D.S., *Journal of Physics D: Applied Physics*, Vol. 11, Section L1, 1978.
10. Drake, P.W., et al., *Journal of Chemical Physics*, Vol. 67, 1977, p. 1969.
11. Berne, B.J. and Pecora, R., "Dynamic Light Scattering," John Wiley and Sons, New York, 1976, p. 182.
12. Lee, W.I. and Schurr, J.M., *Chemical Physics Letters*, Vol. 23, 1973, p. 603.
13. Caroline, D. and Jones, G., *American Physical Society. Bulletin*, Vol. 23, 1978, p. 272.
14. Jackson, D.A., et al., *Journal of Physics C: Solid State Physics*, Vol. 6, Section L55, 1973.
15. Cohen, J., Sankur, V. and Pines, D.J., *Journal of Chemical Physics*, Vol. 67, 1977, p. 1436.
16. Fleury, P.A. and Boon, J.P., *Advances in Chemical Physics*, Vol. 24, 1973, p. 1.
17. Mountain, R.D., *Reviews of Modern Physics*, Vol. 38, 1966, p. 205.
18. Hertzfeld, K.F. and Litovitz, T.A., "Absorption and Dispersion of Ultrasonic Waves," Academic Press, New York, 1959.
19. Lac, P.H., Schoen, P.E. and Chu, B., *Journal of Chemical Physics*, Vol. 64, 1976, p. 3547.
20. Champion, C.W. and Jackson, D.A., *Molecular Physics*, Vol. 31, 1976, p. 1159.

21. Lindsay, S.M., Adshead, A. and Shepherd, I.W., *Polymer*, Vol. 18, 1977, p. 862.
22. Huang, Y.Y., et al., in "Light Scattering in Solids," Proceedings of the International Conference in Paris, 1971, p. 488; also *Flammarion*, 1971.
23. Mitchell, R.S. and Guillet, J.E., *Journal of Polymer Science. Part A-2; Polymer Physics*, Vol. 12, 1974, p. 713.
24. Coakley, R.W., et al., *Journal of Applied Physics*, Vol. 47, 1976, p. 4271.
25. Sandercock, J.R., in "Light Scattering in Solids," Proceedings of the International Conference in Paris, 1971, p. 9; also *Flammarion*, 1971.
26. Dil, J.G. and Brody, E.M., *Physical Review B (Solid State)*, Vol. B14, 1976, p. 5218.
27. Sandercock, J.R., *American Physical Society. Bulletin*, Vol. 23, 1978, p. 387.
28. Szymanski, H.A., ed., "Raman Spectroscopy," Plenum Press, New York, 1967.
29. Craver, C.D., ed., "Polymer Characterization-Interdisciplinary Approaches," Plenum Press, New York, 1971.
30. Schaufele, R.F., *Journal of Chemical Physics*, Vol. 49, 1968, p. 4168.
31. Peticolas, W.L., et al., *Applied Physics Letters*, Vol. 8, 1971, p. 87.
32. Dlugosz, J., et al., *Polymer*, Vol. 17, 1976, p. 471.
33. Hsu, S.L. and Krimm, S., *Journal of Applied Physics*, Vol. 48, 1977, p. 4018.
34. Reneker, D.H. and Fanconi, B., *Journal of Applied Physics*, Vol. 46, 1975, p. 4144.
35. Fanconi, B. and Crissman, J., *Journal of Polymer Science. Part B: Polymer Letters*, Vol. 13, 1975, p. 421.
36. Hartley, A., et al., *Polymer*, Vol. 17, 1976, p. 355.
37. Hsu, S.L., Krimm, S., Krause, S. and Yeh, G.S.Y., *Journal of Polymer Science. Part B: Polymer Letters*, Vol. 14, 1976, p. 195.
38. Rabolt, J.F. and Fanconi, B., *Journal of Polymer Science. Part B: Polymer Letters*, Vol. 15, 1977, p. 121.
39. Rabolt, J.F. and Fanconi, B., *Polymer*, Vol. 18, 1977, p. 1258.
40. Hartley, A.J., et al., in Proceedings of the 5th International Conference on Raman Spectroscopy, Schulz, Freiberg, 1976, edited by E.D. Schmid, Plenum Press, p. 496.
41. Tasumi, M. and Shimanouchi, T., *Journal of Molecular Spectroscopy*, Vol. 9, 1962, p. 261.
42. Schachtschneider, J.H. and Snyder, R.G., *Spectrochimica Acta*, Vol. 19, 1963, p. 85, and also Vol. 19, 1963, p. 117.
43. Lippert, J.L. and Peticolas, W.L., *National Academy of Sciences. Proceedings*, Vol. 68, 1971, p. 1572.
44. Larsson, K., *Chemistry and Physics of Lipids*, Vol. 10, 1973, p. 165; and Larsson, K. and Rand, P., *Biochimica et Biophysica Acta*, Vol. 326, 1973, p. 245.
45. Boerio, F.J. and Koenig, J.L., *Journal of Chemical Physics*, Vol. 52, 1970, p. 3425.
46. Koenig, J.L. and Tabb, D.L., *Journal of Macromolecular Science. Part B. Physics*, Vol. B9, 1974, p. 141.
47. Peterlin, A., et al., *Journal of Polymer Science. Part B: Polymer Letters*, Vol. 9, 1971, p. 583.
48. Gaber, B.P. and Peticolas, W.L., *Biochimica et Biophysica Acta*, Vol. 465, 1977, p. 260; Priest, R.G. and Sheridan, J.P., in "Liquid Crystals and Ordered Fluids," edited by J.F. Johnson and R.S. Porter, Plenum Press, New York, 1978, p. 209.
49. Wu, C.K. and Nicol, M., *Journal of Chemical Physics*, Vol. 58, 1973, p. 5150; and *Chemical Physics Letters*, Vol. 24, 1974, p. 395.
50. Schoen, P.E., Priest, R.G., Sheridan, J.P. and Schnur, J.M., *Nature*, Vol. 270, 1977, p. 412.

#### DISCUSSION

*R. A. DASKIVICH, General Motors Research Laboratories:* I was happy to see that at the end of the talk you brought up the subject of a material that is of some interest in engineering -- polyethylene. In working with this material, what approximately would be your signal to noise ratio, or the effect of signal to noise ratio that you have to play with?

*J. M. SCHNUR:* We are working with molecular weights ranging from 16,000 to about one million. We are really concerned about purity in specifying material properly. In the materials that we annealed for a very long time, some decomposition occurred although the DSC gave us purities of 99.5% which is bringing our signal to noise ratio down to about 3 to 4 for these low frequency modes. However, in the French samples which were not annealed, we found some very interesting characteristics. We were able to get a signal to noise ratio of 20 to 100 with the interferometer coupled to the double monochromator. The signal counts were quite low and we had to count for a long time, but the signal to noise ratio was quite good. If we do not use the interferometer, in both cases we do not see anything at all. We are enhancing contrast from  $10^{12}$  to  $10^{13}$  with the double monochromator by itself, to about  $10^{17}$  with the interferometer coupled in there; that is,  $10^5$  times increase in contrast.

**DAT  
FILM  
0-8**